MICROCOPY RESOLUTION TEST CHART
NATIONAL BUREAU OF STANDARDS-1963-A

ADA132406

FIELDS AND CURRENTS AND CHARGES ON OBSTACLES IN A PARALLEL-PLATE SIMULATOR AT SELECTED FREQUENCIES AND WITH PULSE EXCITATION

T. T. Wu, et al.

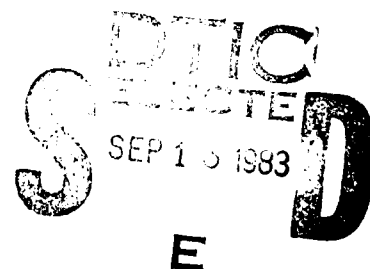Gordon McKay Laboratory
Harvard University
Cambridge, MA 02138

August 1983

Final Report

DTIC
SELECTED
SEP 1 5 1983

E

AIR FORCE WEAPONS LABORATORY
Air Force Systems Command
Kirtland Air Force Base, NM   87117

DTIC FILE COPY

83   09   12   046

This final report was prepared by the Gordon McKay Laboratory, Cambridge, Massachusetts, under Contract F29601-81-K-0010, Job Order 37630143 with the Air Force Weapons Laboratory, Kirtland Air Force Base, New Mexico. William D. Prather (NTAA) was the Laboratory Project Officer-in-Charge.

When Government drawings, specifications, or other data are used for any purpose other than in connection with a definitely Government-related procurement, the United States Government incurs no responsibility or any obligation whatsoever. The fact that the Government may have formulated or in any way supplied the said drawings, specifications, or other data, is not to be regarded by implication, or otherwise in any manner construed, as licensing the holder, or any other person or corporation; or as conveying any rights or permission to manufacture, use, or sell any patented invention that may in any way be related thereto.

This report has been authored by a contractor of the United States Government. Accordingly, the United States Government retains a nonexclusive, royalty-free license to publish or reproduce the material contained herein, or allow others to do so, for the United States Government purposes.

This report has been reviewed by the Public Affairs Office and is releasable to the National Technical Information Services (NTIS). At NTIS, it will be available to the general public, including foreign nations.

If your address has changed, if you wish to be removed from our mailing list, or if your organization no longer employs the addressee, please notify AFWL/NTAA, Kirtland AFB, NM 87117 to help us maintain a current mailing list.
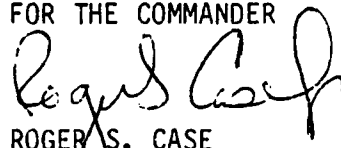
This technical report has been reviewed and is approved for publication.

WILLIAM D. PRATHER
Project Officer

DAVID W. GARRISON
Lt Col, USAF
Chief, Applications Branch

FOR THE COMMANDER

ROGER S. CASE
Lt Col, USAF
Chief, Aircraft & Missile Division

REPORT DOCUMENTATION PAGE		READ INSTRUCTIONS BEFORE COMPLETING FORM
1. REPORT NUMBER AFWL-TR-83-45	2. GOVT ACCESSION NO. AD-A132406	3. RECIPIENT'S CATALOG NUMBER
4. TITLE *(and Subtitle)* FIELDS AND CURRENTS AND CHARGES ON OBSTABLES IN A PARALLEL-PLATE SIMULATOR AT SELECTED FREQUENCIES AND WITH PULSE EXCITATION		5. TYPE OF REPORT & PERIOD COVERED Final Report — 6. PERFORMING ORG. REPORT NUMBER
7. AUTHOR(s) T. T. Wu H. M. Shen M. Krook R. Bansal R. W. P. King M. Owens		8. CONTRACT OR GRANT NUMBER(s) F29601-81-K-0010
9. PERFORMING ORGANIZATION NAME AND ADDRESS Gordon McKay Laboratory Harvard University Cambridge, MA 02138		10. PROGRAM ELEMENT, PROJECT, TASK AREA & WORK UNIT NUMBERS 64711F/37630143
11. CONTROLLING OFFICE NAME AND ADDRESS Air Force Weapons Laboratory (NTAA) Kirtland Air Force Base, NM 87117		12. REPORT DATE August 1983
		13. NUMBER OF PAGES 54
14. MONITORING AGENCY NAME & ADDRESS*(if different from Controlling Office)*		15. SECURITY CLASS. *(of this report)* Unclassified
		15a. DECLASSIFICATION/DOWNGRADING SCHEDULE

16. DISTRIBUTION STATEMENT *(of this Report)*

Approved for public release; distribution unlimited.

17. DISTRIBUTION STATEMENT *(of the abstract entered in Block 20, if different from Report)*

18. SUPPLEMENTARY NOTES

19. KEY WORDS *(Continue on reverse side if necessary and identify by block number)*

Harvard model simulator	Dual measurement procedure
Rhombic simulator	Quasi-traveling-wave expansion method
Continuous-wave and pulse excitation	
Electric field in working volume	
Voltage, current and electric-field pulse sequences	

20. ABSTRACT *(Continue on reverse side if necessary and identify by block number)*

This final report summarizes the results of a 2-year study performed at Harvard University to determine the properties of the Harvard model simulator at selected frequencies and under pulse excitation. The continuous-wave (CW) study is completed with measurements at intermediate frequencies; a novel series apron device is developed to improve the performance in this frequency range. The pulse study begins with a theoretical and experimental investigation of the simpler rhombic simulator, and concludes with an investigation of the

(over)

DD FORM 1473 EDITION OF 1 NOV 65 IS OBSOLETE
1 JAN 73

20. ABSTRACT (Continued).

cont ➤ Harvard parallel-plate simulator. Both the rhombic and the metal-plate simulators exhibit unexpected complications which require further study. Each feature is examined individually and the sources of the many parasitic pulses are determined. Methods for eliminating the undesired pulses are presented, along with a new experimental technique to reduce the systematic interference and a new theory to solve for the current in the time domain.

Accession For	
NTIS GRA&I	☒
DTIC TAB	☐
Unannounced	☐
Justification	
By	
Distribution/	
Availability Codes	
Dist	Avail and/or Special
A	

SUMMARY

When a nuclear explosion occurs in the atmosphere, a powerful outward-traveling pulse of electromagnetic radiation is generated that can have dangerous effects on aircraft or missiles in its path. To study these effects and the means to avoid them, very large simulators have been constructed in which aircraft and missiles are exposed to electromagnetic pulses. An extensive investigation to determine the properties of a model simulator at selected frequencies and under pulse operation has been conducted at Harvard University for a number of years. This final report summarizes the results for the two-year period from February 2, 1981 through May 1, 1983.

The electric field in the working volume of the simulator was measured at intermediate frequencies (with particular attention to the notch frequency) and means were devised for eliminating both the notch and the residual, quite large standing-wave ratio. (Comparable measurements at low and high frequencies had been completed earlier.) The effects of a high standing-wave field with a deep minimum or notch on the currents and charges induced on a cylindrical metal object in the simulator were then determined. This completed the continuous-wave (CW) study. A comprehensive theoretical and experimental study of the rhombic simulator under pulse operation was then carried out, as a preparation for studying the Harvard metal-plate simulator when excited by a single voltage impulse. The experimental study of the Harvard model simulator which followed exhibited properties similar to those of the rhombic simulator. In particular, a number of unexpected complications in the electric-field pulse sequence were observed which required further study. A careful individualized examination of these unusual features succeeded in identifying each and providing the means for their elimination, thereby achieving a more nearly uniform electric-field pulse in the simulator. The report also contains a description of a new experimental method, the dual measurements procedure, which greatly reduces the systematic interference inherent in the simulator setup, permits a wider variety of measurements to be taken, and provides notably more accurate results. The report concludes with a section on the newly developed quasi-traveling-wave expansion method for solving the integral equation for the current in a cylindrical conductor, or an electromagnetic pulse (EMP) simulator, in the time domain.

CONTENTS

ILLUSTRATIONS

5

6

I. INTRODUCTION

Very large parallel-plate type structures with tapered input and output ends are used to test the vulnerability of aircraft and missiles to electromagnetic pulses that are supposed to simulate those emanating from nuclear explosions in the atmosphere. Voltage pulses applied at one end of the structure excite current pulses that spread out and travel along the wire-mesh walls, continuously generating a transient electromagnetic field between them. An aircraft under test and located in the "working volume" of a simulator is exposed to a field that is much more complicated than that generated in the absence of the test obstacle because of multiple reflections between the obstacle and the walls of the simulator. Extensive experimental and theoretical investigations have been conducted at Harvard University under AFWL Contract F29601-81-K-0010 during the period February 2, 1981 through February 2, 1983 to provide additional information about the performance of our simulators. A summary of this work follows.

II. CONTINUOUS-WAVE OPERATION OF THE HARVARD EMP SIMULATOR

In order to approximate an electromagnetic pulse propagating outward in the atmosphere at a sufficient distance from a nuclear explosion, the electromagnetic field in a simulator of the guided-wave type, shown in Figure 1, must have the properties of a simple transverse electromagnetic (TEM) wave at each frequency in the entire range involved in the pulse. In particular, the standing-wave ratio (SWR) must be close to unity throughout the volume bounded by the parallel-plate part of the simulator. Extensive measurements made in the Harvard metal-plate model simulator have shown that at both low and high frequencies, the electromagnetic field in the parallel-plate region exhibits a fairly low SWR of the order of two or less (Ref. 1). At low frequencies ($kh \ll 1$), where h is the spacing between the parallel plates, the electromagnetic properties of the simulator are those of the well understood two-conductor transmission line in which TEM waves propagate from the generator to the terminating impedance, radiation from the structure is negligible, and reflections at the junctions of the tapered and parallel-plate sections are insignificant. When the terminating impedance is equal to the characteristic impedance of the structure, the SWR is small and most of the power supplied by the generator is dissipated in the termination. At higher frequencies ($kh > 2\pi$), radiation becomes a dominant instead of negligible property of the structure which now behaves more like an antenna than a transmission line. Significant reflections occur at the junctions of the parallel-plate and tapered sections and at their edges so that only a small fraction of the input power actually reaches the terminating load; most of it is radiated. The representation of the field between the parallel plates by a TEM mode becomes inadequate and higher modes are required. The low SWR in the parallel-plate region in the high-frequency range is due to strong radiation loading when the plate spacing h is greater than a wavelength.

At intermediate frequencies, when $kh \sim 2\pi$, neither the transmission-line termination nor the radiation loading is effective in maintaining a low SWR in the parallel-plate region. The power radiated and the power dissipated in the terminating resistance are of comparable magnitude and the effective condition of match deteriorates so that a large SWR is observed. Under special circumstances at certain critical frequencies and locations, unusually deep minima occur in the standing-wave pattern. The ratio of an adjacent maximum to such
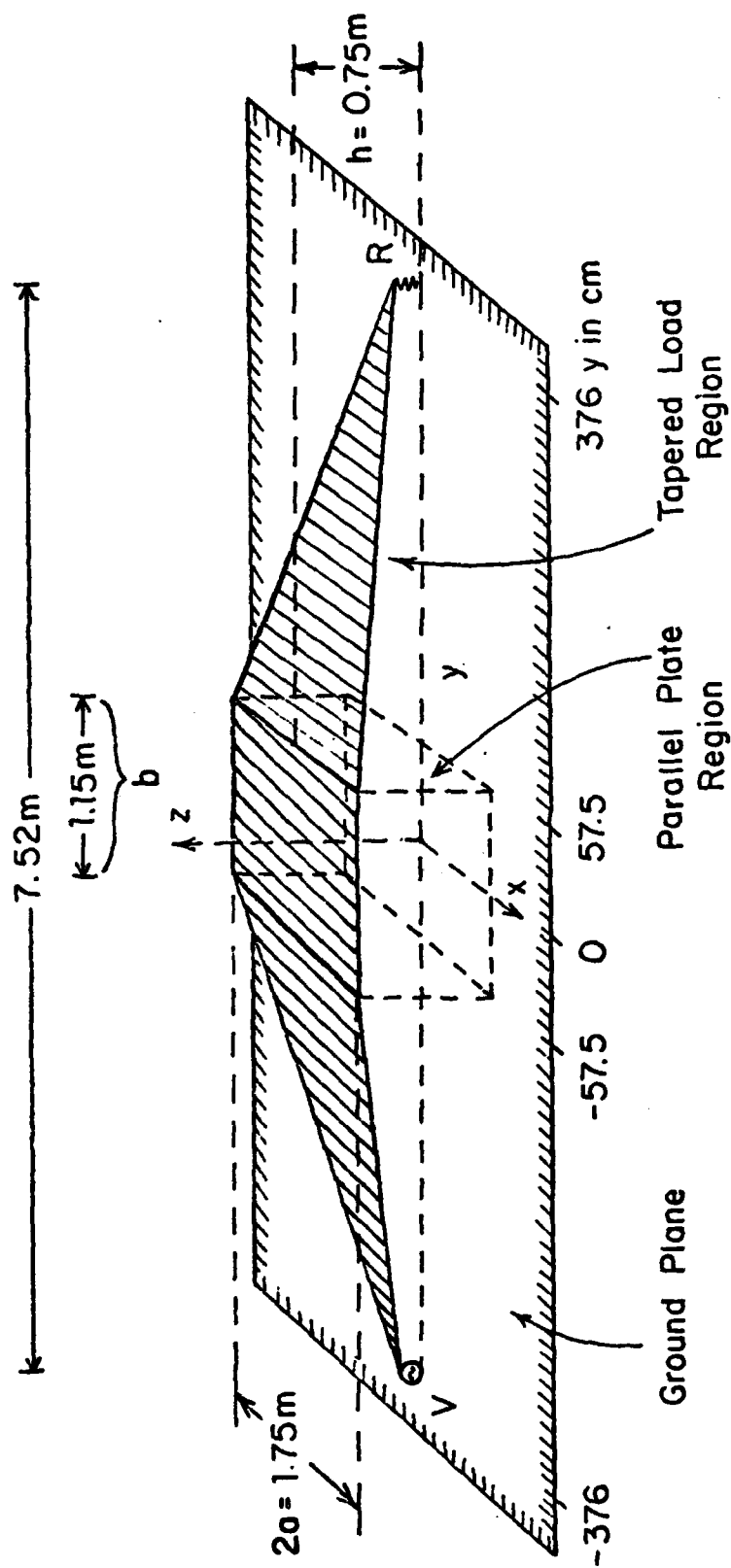
8

Figure 1. The Harvard model simulator adjusted for intermediate frequencies; f = 271 MHz.

a deep minimum may be as large as 25. An example of such a deep minimum is shown in Figure 2 in terms of the measured magnitude of the transverse magnetic field $H_x(x,y,z)$ in the parallel-plate region at the point $x = -10.5$, $y = 8.5$, $z = 0$ cm as a function of frequency. It is seen that there is a succession of minima and maxima, but only one very deep minimum at $f = 264$ MHz. This has been called the notch. At another location in the simulator, the frequency for and the depth of the deepest minimum are different. The deepest minimum for $E_z(x,y,z)$ occurs at $f = 271$ MHz.

An experimental investigation has been conducted to study the electric field throughout the parallel-plate region of the Harvard model simulator at $f = 271$ MHz (Ref. 2). Attention was directed toward determining the origin of the deep minimum and devising means for eliminating it and reducing the otherwise quite high SWR (generally of the order of 5 to 6 with $f = 271$ MHz and $h = 75$ cm). It is shown that the standing waves are due primarily to the TEM mode which experiences reflections before it reaches the termination. The deep minimum or notch in the electric field is due to the almost complete cancellation of the imaginary part of the standing TEM wave by the imaginary part of the standing transverse magnetic (TM) wave near the zero of the real part of the standing TEM wave. Thus, even the complete elimination of the TM mode can do no more than remove the notch with a negligible effect on the residual, quite large TEM standing wave. Accordingly, a novel device called a series apron (Fig. 3) has been developed and tested which provides a reflected TEM wave from the tapered region that effectively cancels much of the otherwise reflected TEM wave to leave a greatly reduced SWR (near two over the entire mid-frequency range) in the parallel-plate region. The structure consists of a trapezoidal plate located parallel to and 5 cm below the triangular plate to form a sleeve or apron with an open end toward the parallel-plate region, a closed end toward the load. The length of the plate and its location were varied to determine the most effective configuration. Strictly, a similar folded section should be located on the outer as well as on the inner surface of the triangular plate, as suggested in broken line in Figure 3, since a significant fraction of the total surface current on the triangular plate is on its outer surface. Measurements have shown, however, that the simpler structure is highly effective. The device has the advantage that, when properly adjusted, it greatly reduces the SWR at the intermediate frequencies, yet has little effect on the high- and low-frequency ends of the
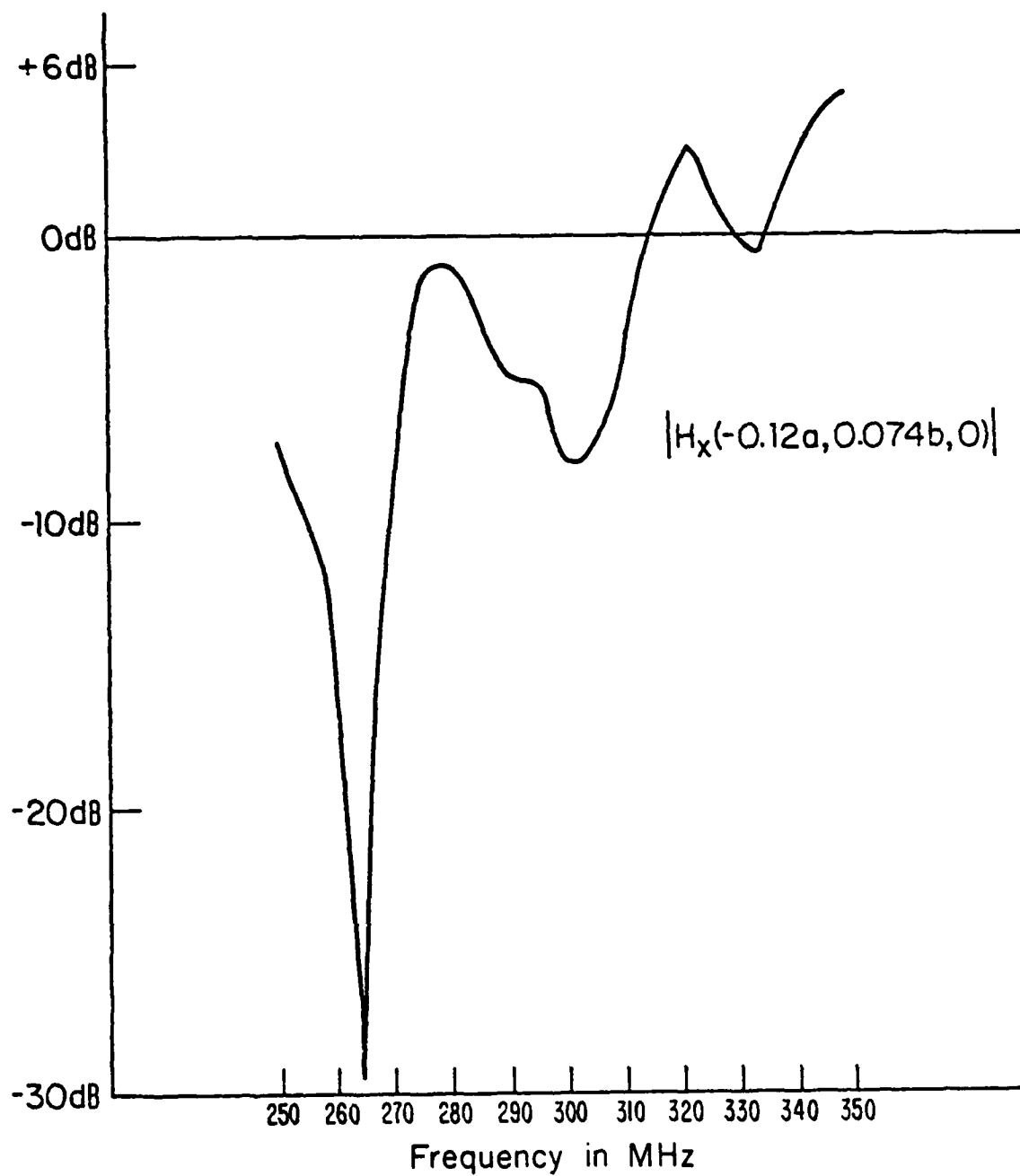
Figure 2. Measured magnitude of the transverse magnetic field at a fixed position in the working volume of the Harvard model simulator as a function of frequency; 2a = 175 cm, b = 114.8 cm, h ≈ 75 cm.
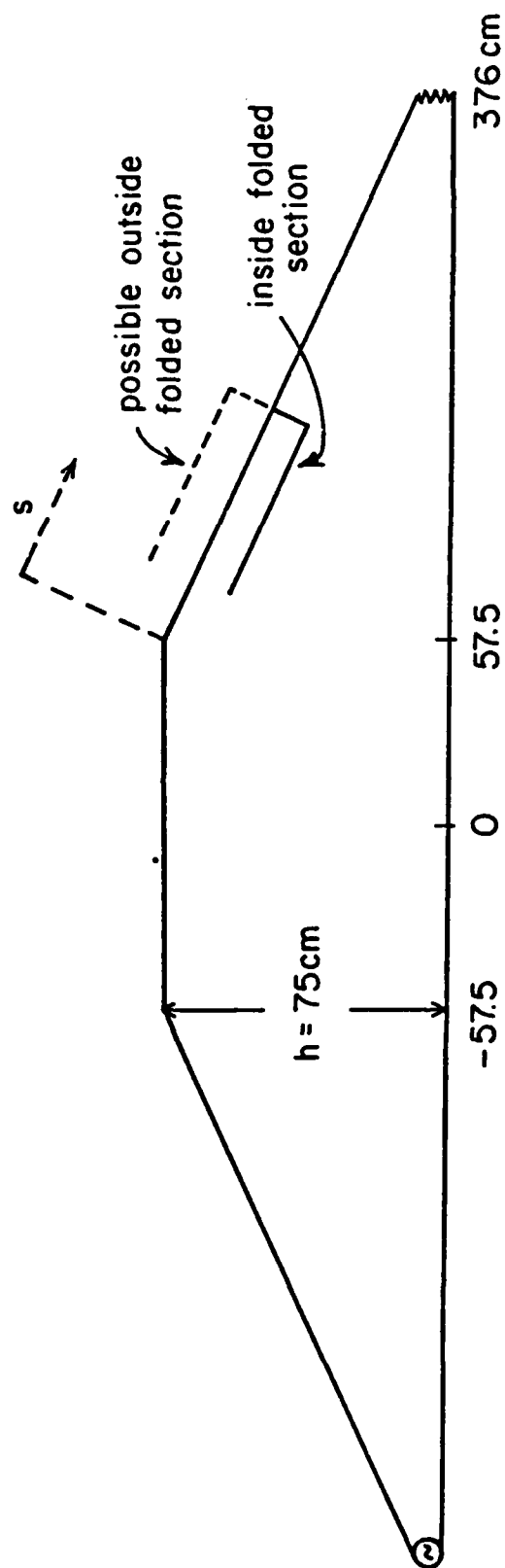
11

Figure 3. Cross section of Harvard simulator with sleeve or apron sections.

spectrum. It simultaneously eliminates the deep minimum or notch. In this manner undesired reflections have been greatly reduced so that the field in the simulator has been brought much closer to the required traveling-wave distribution characteristic of the field propagating outward from a nuclear explosion.

The importance of this accomplishment is demonstrated by a comparison of the measured currents and charges induced on electrically thick cylinders when located in the simulator at different locations in a high standing-wave field and the corresponding quantities when the inducing field is a plane traveling TEM wave. Earlier studies have shown that the distribution of the surface density of charge is particularly sensitive to the nature of the incident field. Accordingly, measurements have been made of the density of charge on the surface of a tubular metal cylinder with $ka_c = 0.916$ when located at successively different points in a high standing-wave field in the simulator (Ref. 3). The measurements were made specifically at the notch frequency, $f = 271$ MHz, when an extremely deep minimum exists in the standing wave. Theoretical distributions of the surface charge density when the exciting field is an ideal traveling plane wave were computed using the theory and program of C. C. Kao (Ref. 4). A comparison of the theoretical and experimental results shows that when an electrically large obstacle of the simplest form is located in a standing wave that includes TEM and TM waves with a deep minimum, the distribution of the induced surface density of charge not only differs from that induced by a traveling TEM wave, but depends on the location of the cylinder in the standing wave. With reference to Figure 4, it may have the form of a traveling wave on the shadowed side ($\theta = 0$ degrees) and a standing wave on the illuminated side ($\theta = 180$ degrees) when the rear of the cylinder is at a minimum ($y_c = 28.8$ cm) or precisely the reverse when the center of the cylinder is at the minimum ($y_c = 45$ cm). The amplitude of the charge density halfway up the cylinder on its shadowed side may vary by a factor as large as 4 as the cylinder is moved from a location with the minimum in the exciting field at the rear ($y_c = 28.8$ cm) to a location with the minimum at the front ($y_c = 61.7$ cm).

As already mentioned in the introduction, when an obstacle is placed in the parallel-plate region of an EMP simulator, it cannot be assumed that the exciting field is that obtaining in the simulator in the absence of the obstacle. Owing to the coupling between the obstacle and the simulator, the
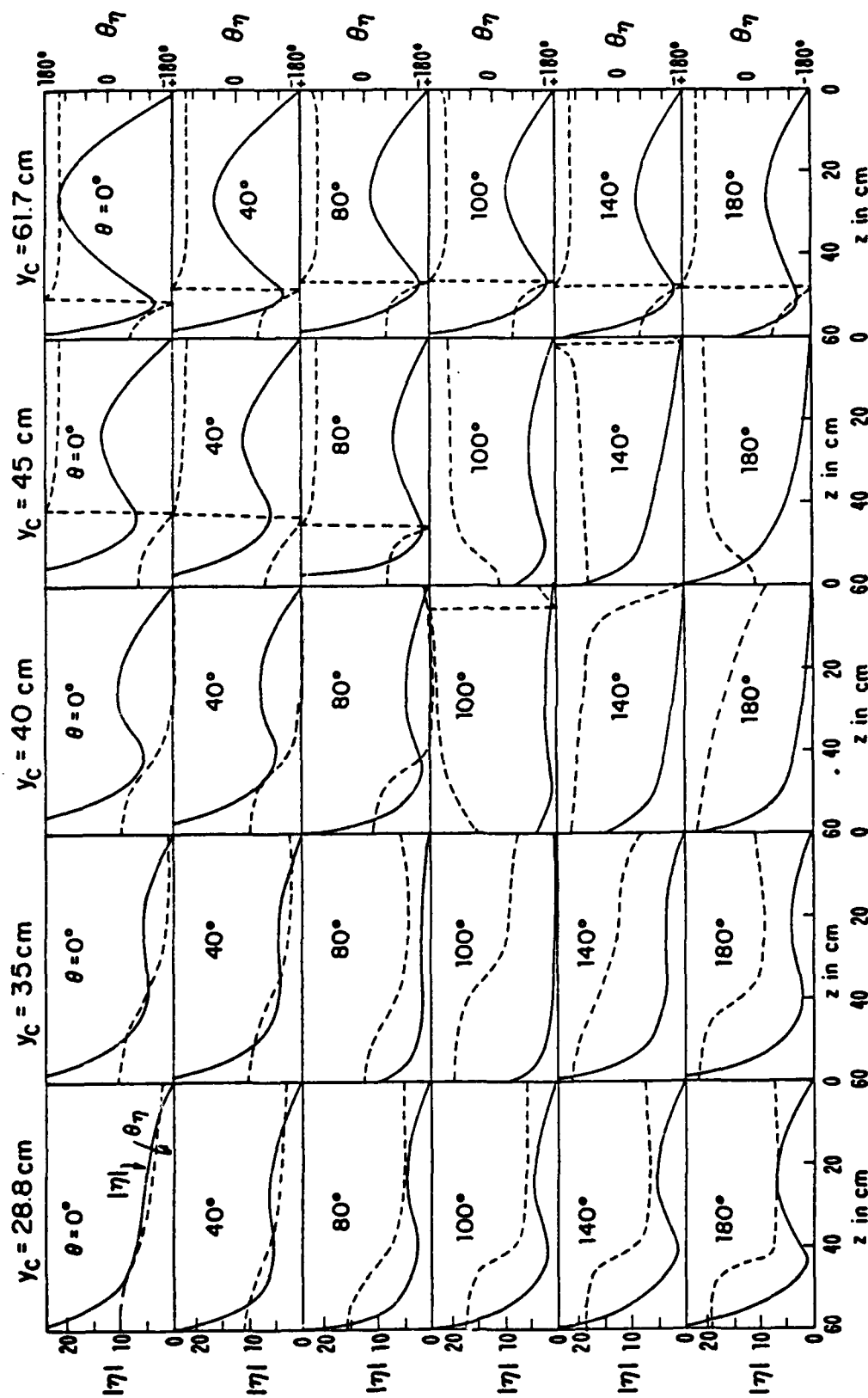
Figure 4. Measured surface density of charge on cylinder with $ka_c = 0.916$, $kh_c = 3.37$ at five locations in Harvard model simulator.

14

distributions of current and charge on the simulator are modified so that the field they generate is no longer the same as when the obstacle is removed. This interaction is relatively small when the obstacle is a thin vertical cylinder because collinear coupling is weak. It becomes more and more significant as the horizontal extent of the obstacle and its proximity to the surfaces of the simulator are increased. In the study reported in Reference 3, the collinear coupling with the vertical currents is small, and the coupling to the horizontal transverse currents near the open end of the cylinder is probably not of primary significance. This concludes the part of the investigation concerned with the properties of the model simulator at selected frequencies.

III. THE RHOMBIC SIMULATOR UNDER PULSE EXCITATION - EXPERIMENTAL STUDIES

With the completion of the continuous-wave study of the Harvard model simulator, attention was directed to studying its properties under pulse excitation. Since the structure of the Harvard model simulator is complicated, it is difficult to develop an adequate theory for the parallel and triangular plates as a unit. To gain an understanding of the basic physical principles that underlie the pulse operation of a traveling-wave simulator, it was necessary to simplify its structure so that it could be analyzed in general and not only under low-frequency conditions. The configuration selected is a thin-wire, two-conductor rhombic antenna, the conductors of which, in effect, lie along the edges of a volume like that occupied by a wire-mesh or metal-plate simulator (Fig. 5). A principal advantage of the rhombic simulator is the localization of the currents and charges in the electrically thin tubular conductors and the consequent relative simplicity in their determination analytically. Once the distributions of current and charge are known, the electromagnetic field in the region bounded by the conductors is readily determined. The same advantage obtains when the simulator is excited by a voltage pulse across the input terminals at one end. The pulses of current that are generated travel along the conductors with a velocity close to that of light so that their progress can be followed with sensors suitably located along the conducting tubes. Pulses reflected by the load can also be observed. The electric field generated in the space bounded by the conductors by radiation from the traveling pulses can be investigated with suitably located sensors. At any given location, the field consists of the sequence of pulses arriving at that location from the various points of reflection and radiation encountered by the pulses of current traveling along the tubular conductors.

The pulse-excited rhombic-wire system is illustrated in Figure 6. The pulse generator is a fast-rise-time solid-state nanosecond impulse generator (AvTech Model AVG-2). The rise time is less than 1 ns, the pulse width is less than 2 ns, the frequency range of the spectrum is from 0 to 500 MHz, and the output amplitude is 250 V with a 50-Ω load. To match the input impedance of the rhombic simulator, use is made of a pulse transformer (AvTech Model AV-133) which provides the required 50 to 150 Ω impedance transformation. The signals are detected by different sensors, as shown in Figure 6, appropriate

Rhombic Wires (Coinciding with the Edges of Tapered Plates)

Tapered Plate
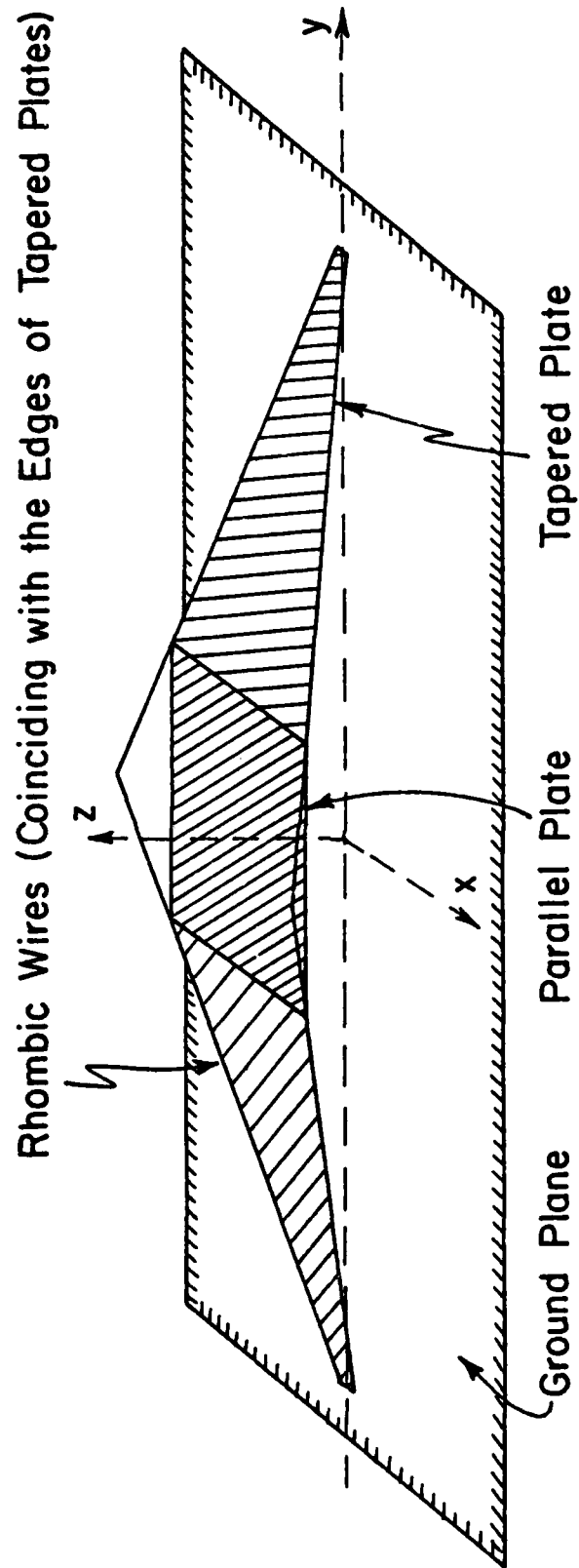
Parallel Plate

Ground Plane

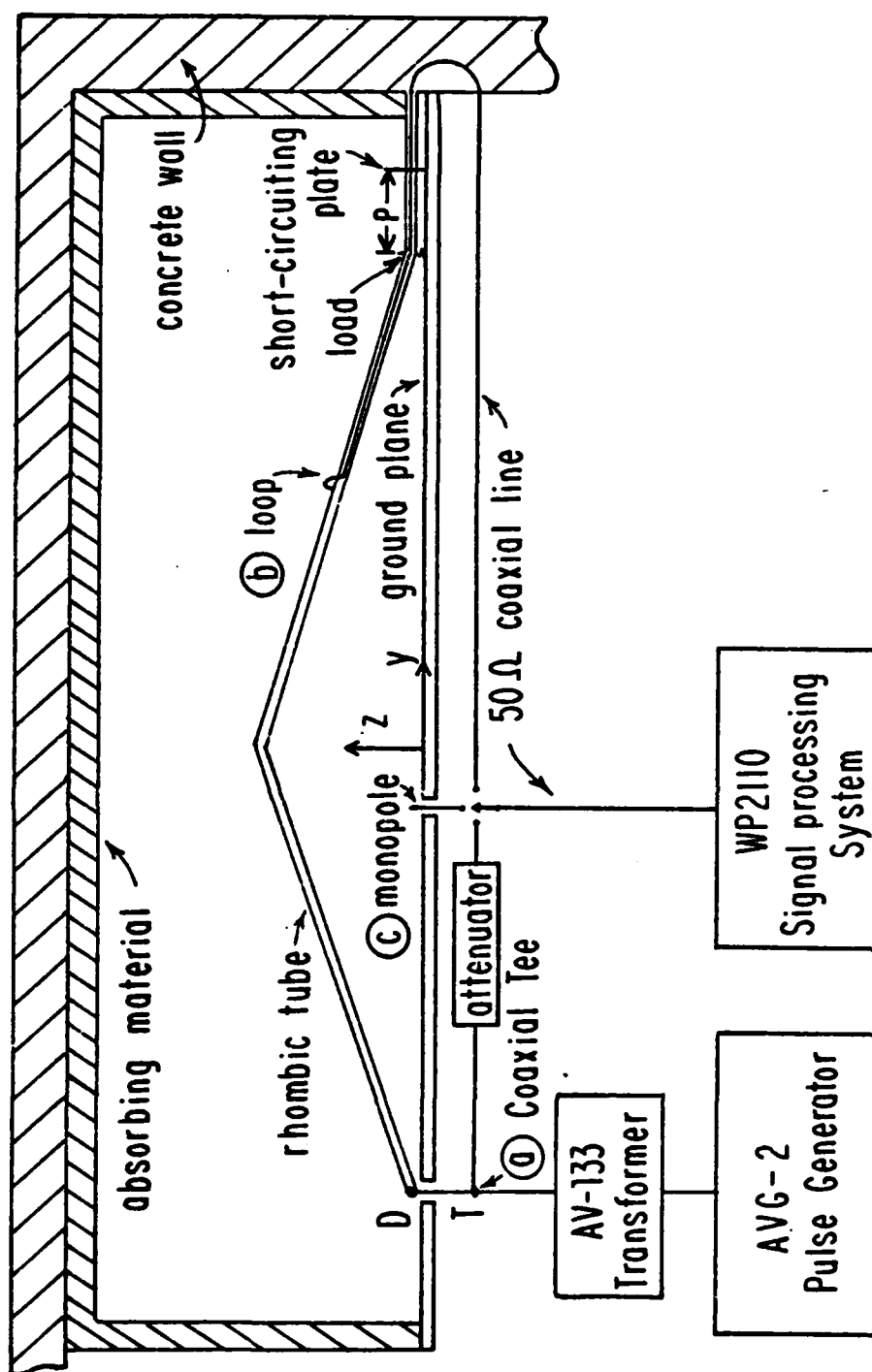Figure 5. The Harvard model simulator coinciding with rhombic simulator.

17

Figure 6. Schematic diagram of rhombic simulator under pulse excitation.

to the signals to be measured. These are the voltage in the coaxial line, the currents along the rhombic wire or tube, and the electric field on the metal ground plane. The signals detected by the sensors are sent to a signal-processing system which has the capability of accepting high-speed transient signals, digitizing and storing them for subsequent data processing (time integral, Fourier transform, etc.). The system (Tektronix Model WP2110 Programmable Digitizer System) includes a waveform acquisition instrument for high-speed signal acquisition, digitizing, and storing of repetitive or single-sweep signals; a graphic computing system (Model 4052) which provides specialized intelligence appropriate to signal processing; and certain peripheral equipment (mass storage, printer, and plotter).

The experimental investigation of the rhombic simulator when excited by an impulse generator led to the following main conclusions (Ref. 5):

(1) When the rhombic conductors are excited by a voltage pulse, the current along them is in the form of a traveling pulse. When such a current pulse travels along the rhombic conductors, the electromagnetic field between them is also a traveling pulse from the source to the load. The waveforms of the three pulses (voltage, current and field) are quite different.

(2) The incident pulse is independent of the load (Fig. 7). Before a reflected pulse arrives (at the center of the working space the reflected pulse has more than a 20-ns delay), the sequences of electromagnetic pulses are totally unaffected by the load. Any attempt to obtain an ideal traveling wave in the entire frequency region by adjusting the load would be futile. Since interest is confined to the incident pulse (in an EMP test only the pulse that arrives first is of interest), the effect of the load is irrelevant.

(3) The two-conductor rhombic antenna used as an EMP simulator has very good wave-guiding characteristics since it provides a very uniform pulse traveling through the middle of the working volume for an EMP test. Figure 8 shows seven pulse sequences in the central working space (-75 cm $\leq y \leq 75$ cm). The amplitudes of the pulses, shown in Figure 9, decrease slightly while the shape remains almost unchanged.

(4) As the incident pulse approaches the load, a second incident pulse develops close to but lagging the first pulse (Fig. 10). There is also a

19
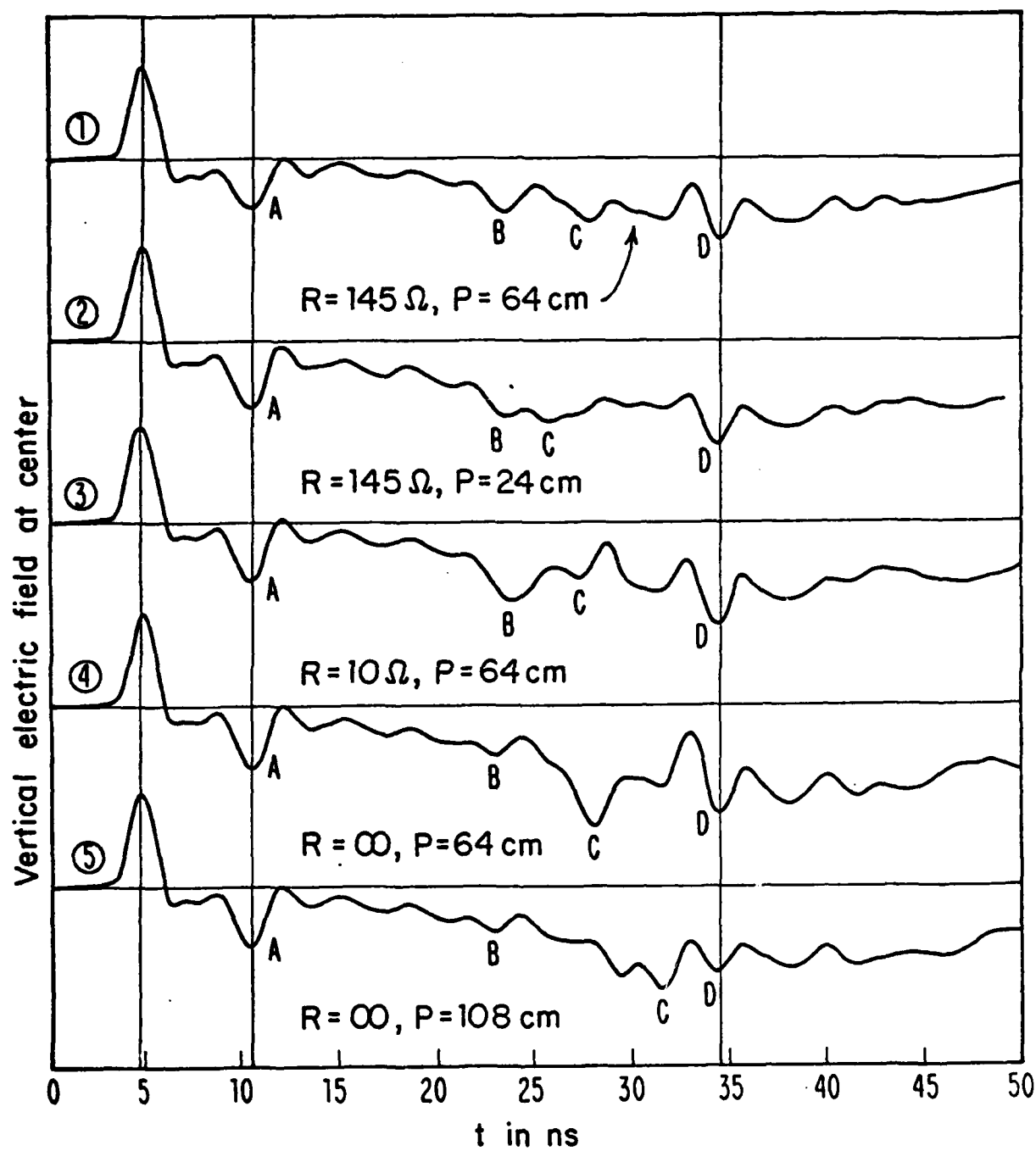
Figure 7. Pulse sequences of vertical electric field on ground plane (x = y = z = 0) in rhombic simulator for different loads.

20

Figure 8. Pulse sequences of vertical electric field in central working space ($x = z = 0$, $-75 < y < 75$ cm) in rhombic simulator; $R = 145$ Ω, $P = 64$ cm.

Figure 9. Distribution of amplitudes of incident pulses in Figure 8.

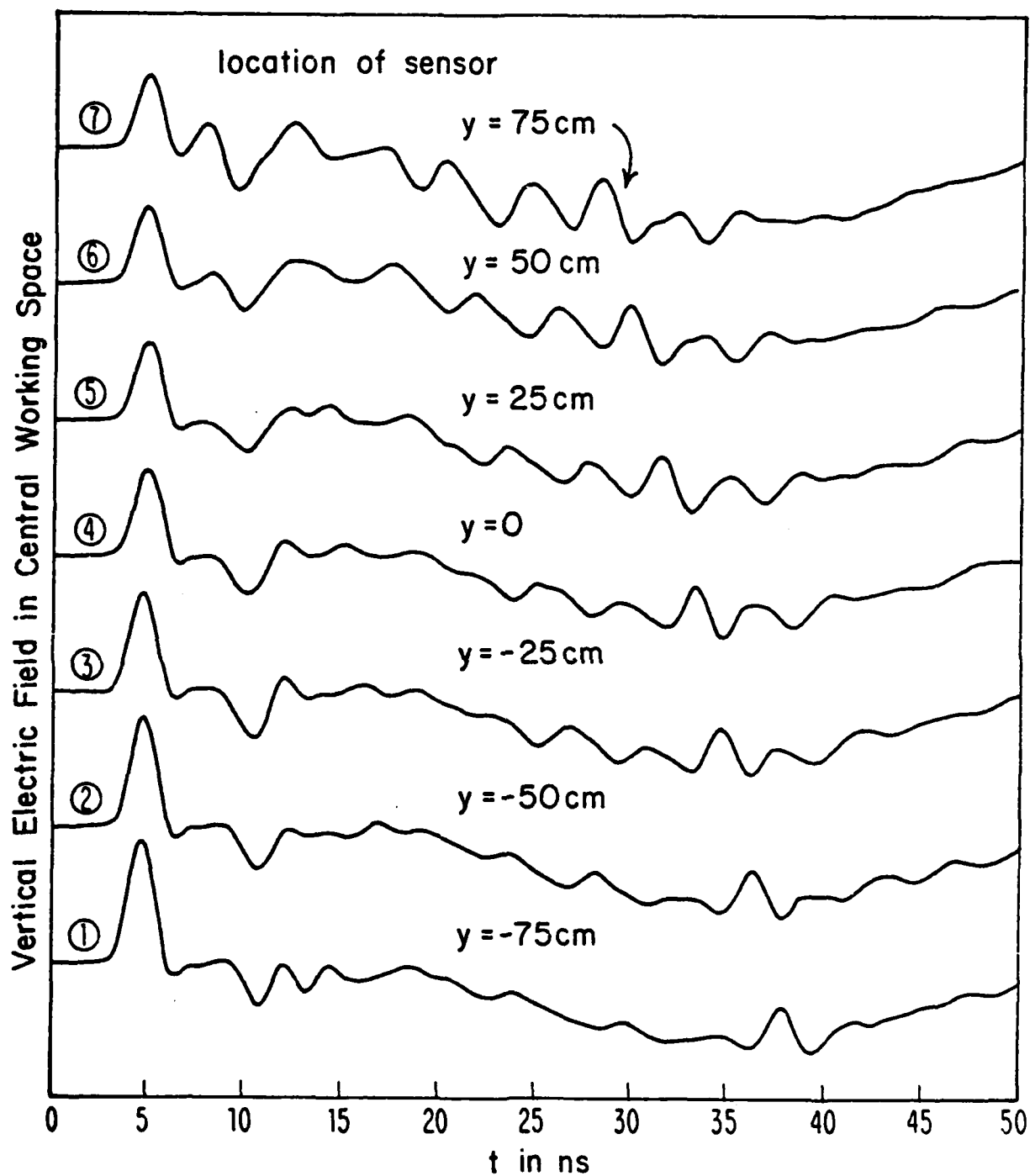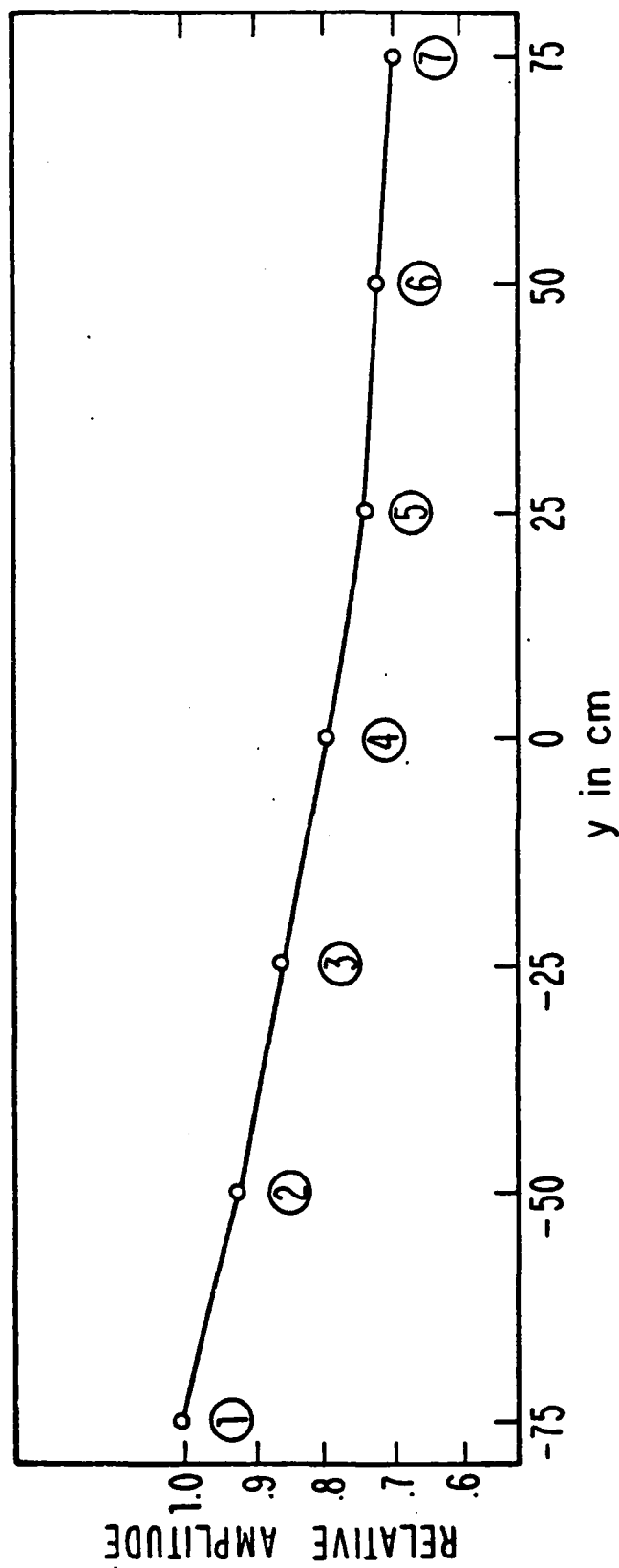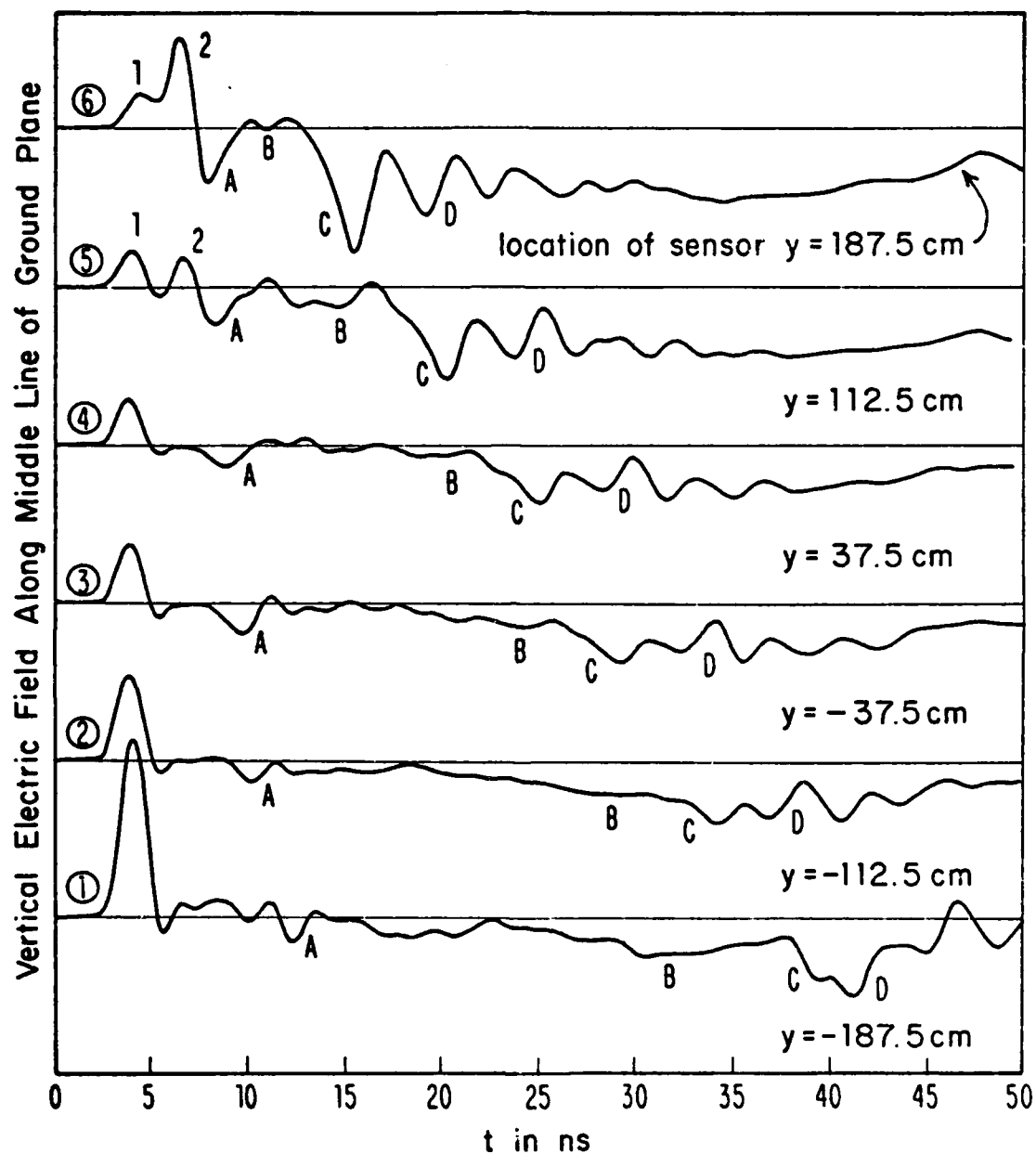Figure 10. Pulse sequences of vertical electric field along middle line of ground plane in rhombic simulator; R = ∞, P = 64 cm.

third and negative pulse, close to the incident pulses, which is not the reflected pulse from the load.

(5) The results obtained with two different excitations (pulse and continuous-wave) are consistent with each other, as shown in Figure 11 for the intermediate frequency f = 416 MHz. Good agreement was also obtained at the low frequency f = 100 MHz.

The experimental investigation of the rhombic simulator excited by an impulse raised a number of important questions. When the rhombic structure is excited by a single pulse, the observed pulse sequences in the electric field are characterized by complications (Fig. 10) which require careful study. As expected, the electric field between the wires near the source is a single pulse with a shape that may differ from that of the initial driving voltage pulse (Fig. 10; curves 1, 2, and 3). However, as this pulse is observed at successive locations across the central region between the wires, a second pulse appears directly behind the first one. It grows larger as it approaches the load end of the simulator. When the load is reached (Fig. 10, curve 6), the second pulse (labeled 2) is actually larger than the first one (labeled 1). Clearly, it is necessary to explain the origin of the second pulse and why it appears only near the load. Following these two incident pulses, a negative pulse (labeled A) is observed which has a time delay that changes linearly with the location of the sensor. Since pulse A cannot be the reflected pulse from the load, the question arises where does it originate? In addition, this sequence of three pulses is superimposed on a slowly changing background signal. Where does it come from? It is also surprising that the width of the observed electric-field pulse does not increase as compared with the width of the voltage pulse at the driving point. An increase in width should be a consequence of the fact that the field contributed by the currents at different locations arrives at slightly different times. To explain this apparent contradiction, it is necessary to consider that there is a weighting factor that affects the contributions to the electric field from currents at different locations. Evidently, the answers to these several questions will be very instructive and essential to acquiring a deeper understanding of what actually occurs along the rhombic structure when it is excited by a single voltage pulse. Answers to all of these questions have been provided in a series of papers (Refs. 6 through 9) which will be discussed in turn.
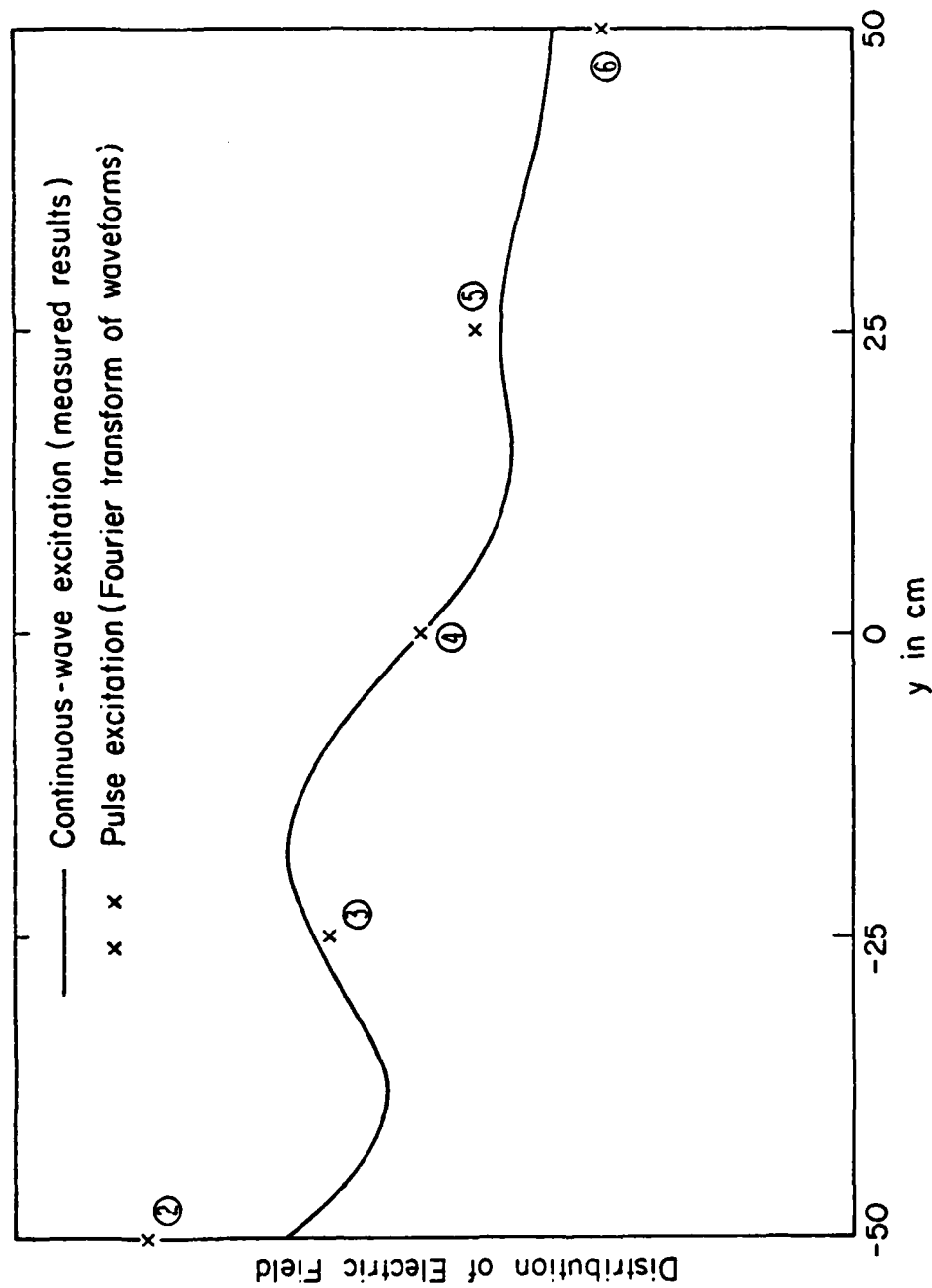
Figure 11. Comparison of distributions of electric field in rhombic simulator for continuous-wave and pulse excitations at intermediate frequency f = 416 MHz.

25

IV. THE RHOMBIC SIMULATOR UNDER PULSE OPERATION - THEORETICAL STUDIES

The theoretical analysis of the rhombic simulator under pulse excitation evaluates the electric-field pulse generated by a current pulse with known shape traveling along the rhombic wires (Ref. 6). The calculated pulse sequences agree extremely well with the measured ones. The electric-field pulse is represented as a superposition of subpulses $e_{i,n}$ which are emitted from the successive segments 1 to n of the front (i = 1) or rear (i = 5) wires. The properties of the subpulses $e_{i,n}$ help to explain why the width of the electric-field pulse does not increase as it progresses and why the second incident pulse does not appear in the front region. A study of Figure 12 and curve I of Figure 13 reveals that the electric-field pulse emitted by the front wires and images is largely due to the subpulses $e_{1,1}$ to $e_{1,4}$ which originate in the parts of the front wires nearest the source. Although their amplitudes are relatively small, they coincide in time so that they add together. Further along the wires, the amplitudes of the subpulses increase, but here they are not coincident in time so that they contribute very little to curve I of Figure 13. Clearly, the relative time shift of the subpulses plays an important role in the formation of the complete electric-field pulse; the amplitudes of the subpulses are relatively less important. The first incident pulse of the electric field is generated primarily by the subpulses of current which come from a relatively small region of the front wires nearest the source. That is why the pulse retains its shape without getting wider. The same is true of the second incident pulse of the electric field which is generated primarily by the currents in a small part of the rear wires and images (see Fig. 12b and curve II in Fig. 13). The second incident pulse does not occur in the forward region of the metal ground plane because the backward subpulses from the rear wire which would have to generate it are non-coincident so that their contributions tend to cancel. In Figure 14 are shown the superpositions of the individual subpulses at the center of the ground plane due to the currents in the eight sections of the front and those of the rear wires. It is seen that, although the amplitudes of the individual subpulses from the rear wires are comparable in magnitude to those from the front wires, their superposition leads to virtually complete cancellation: curve II of Figure 14 shows no pulse.
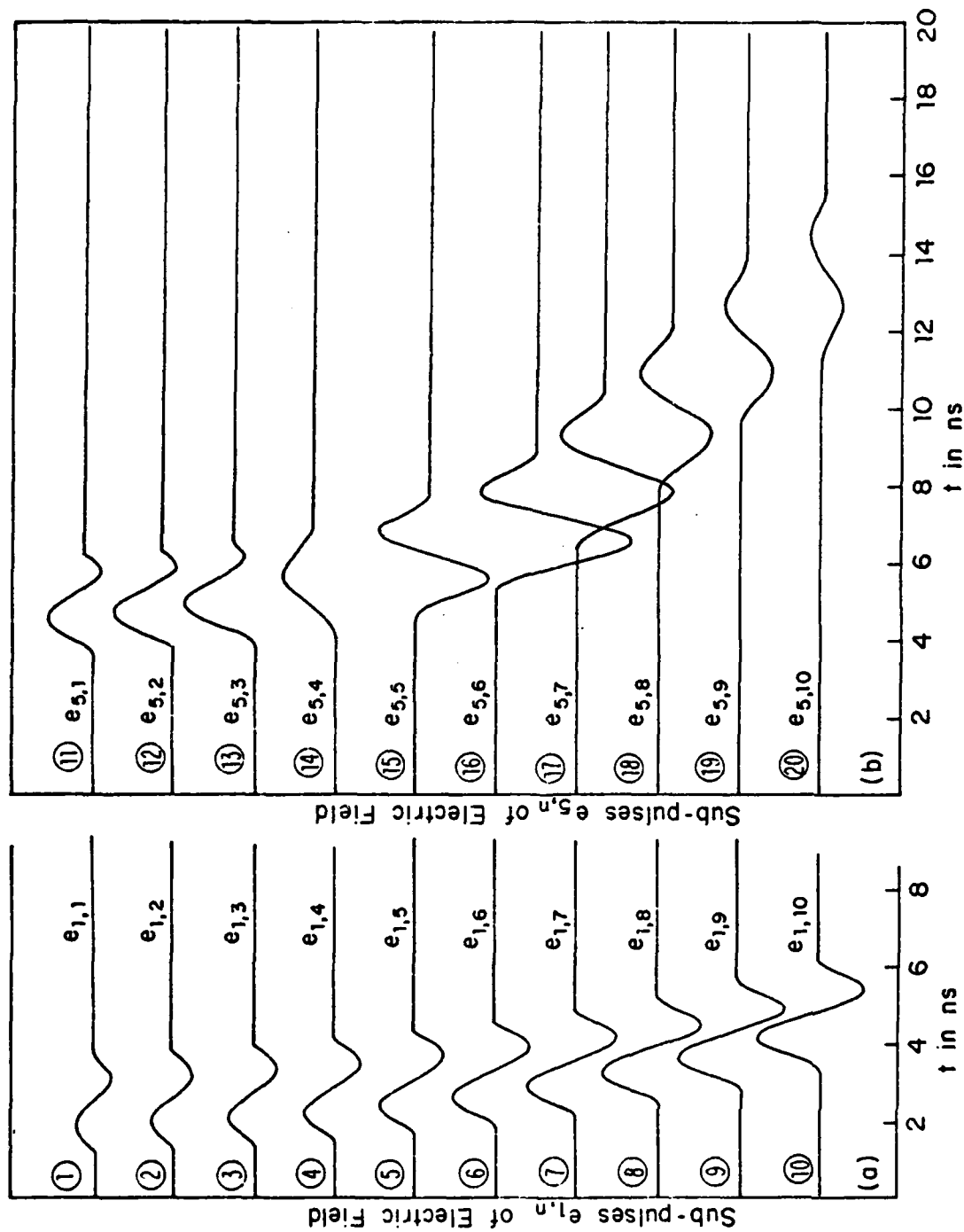
Figure 12. Subpulses of electric field at location V on ground plane originating from: (a) front, and (b) rear rhombic wires.

27
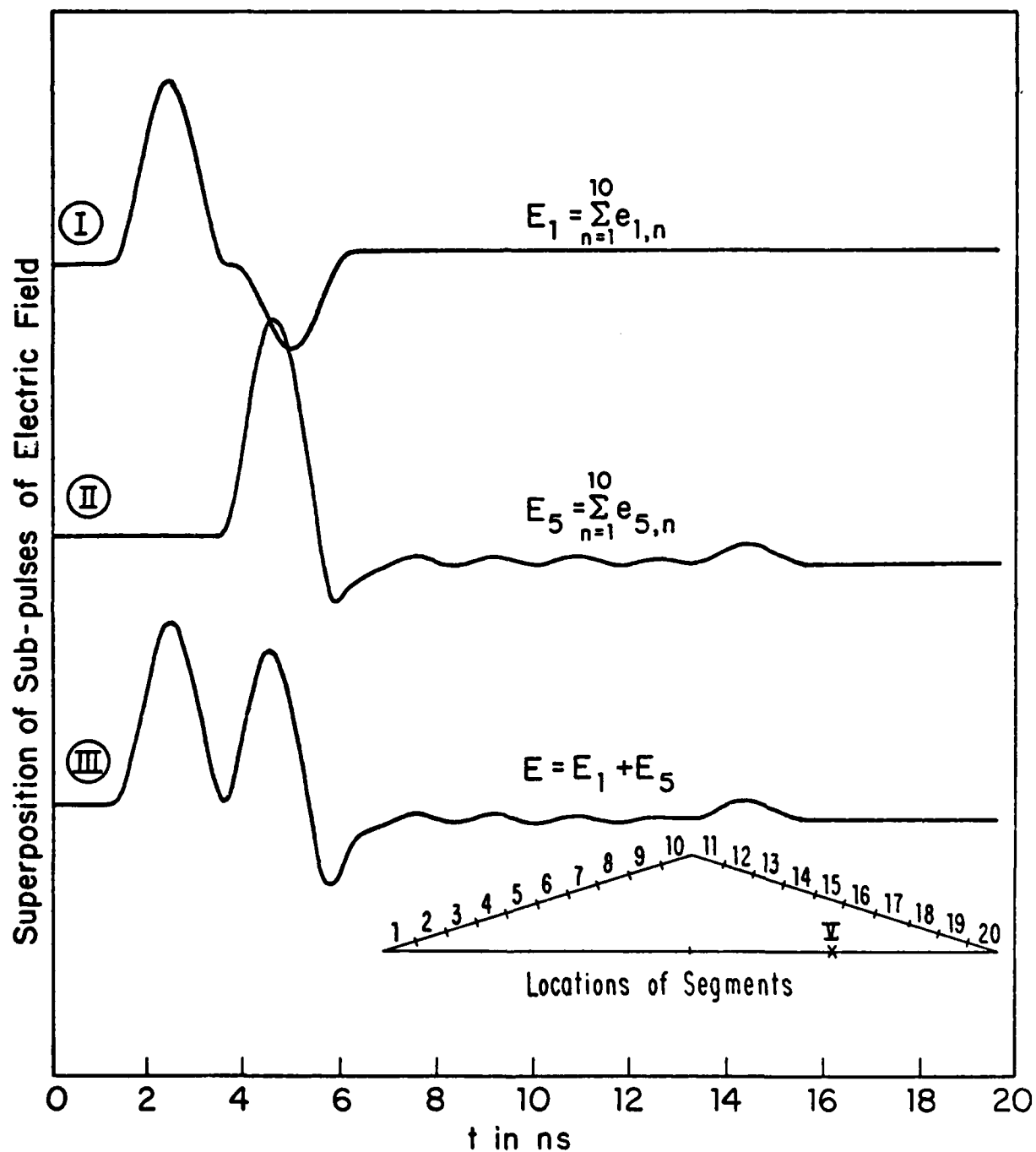
Figure 13. Superposition of subpulses of electric field at location V on
ground plane in rhombic simulator originating from:
(I) front, (II) rear, and (III) all rhombic wires.

28
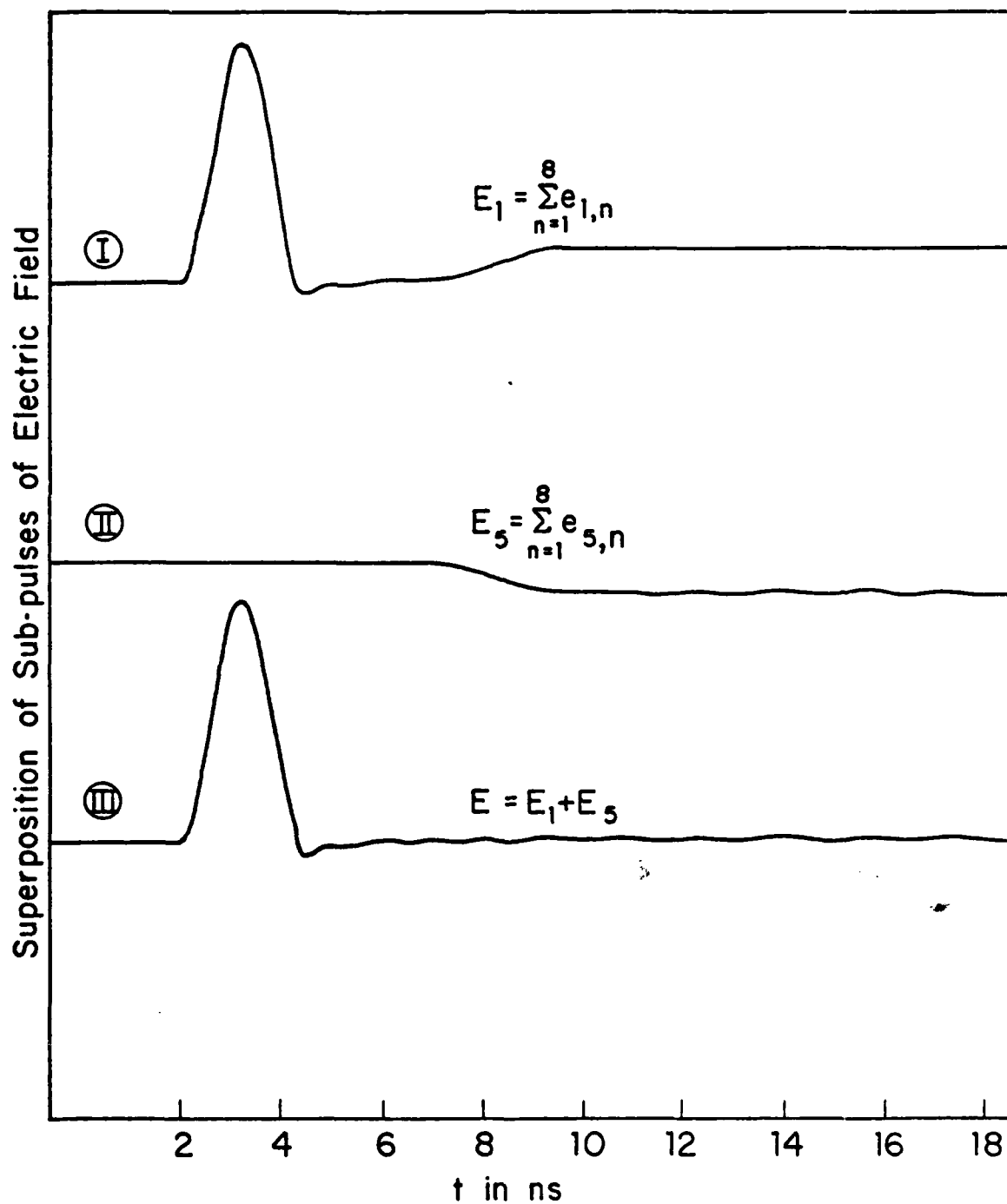
Figure 14. Superposition of subpulses of electric field at center of ground plane (y = 0) in rhombic simulator originating from: (I) front, (II) rear, and (III) all rhombic wires.

Attempts were made to locate the source of the negative pulse A in the rhombic conductors or in the surrounding objects by moving or shielding them individually, but these were unsuccessful. This would seem to indicate that the negative pulse A is a part of the incident pulse sequence. A more complete answer to this question is discussed in Section VII.

V. THE HARVARD EMP SIMULATOR UNDER PULSE EXCITATION

After the detailed study of the characteristics of the rhombic simulator under pulse excitation was completed, the consideration of the Harvard model simulator could be resumed. The investigation of the metal-plate simulator under pulse excitation is very important. It reveals not only how the system actually behaves in an EMP test, but also provides a new tool fc: acquiring additional information about the simulator which is difficult to obtain from CW measurements. Since the pulses reflected from different parts of or objects in the simulator (e.g., metal plates, joints, terminating resistor, etc.) are separated in time, it is possible to identify them in the complex sequence of observed pulses and then to investigate them individually. This permits an individualized study of the effects caused by each object.

Measurements were made of the voltage at the driving point, the current and charge densities on the surfaces of the top plate, and the electric field between the plates in the Harvard EMP simulator (Ref. 7). The Harvard simulator is found to have properties that are very similar to those of the rhombic simulator; this is not a mere coincidence. Since the current on the top metal plate of the Harvard EMP simulator is concentrated near the edges -- which is the location of the conducting tubes in the rhombic simulator -- the two electric fields have quite similar current sources. As in the case of the rhombic simulator, a change in the load in the metal-plate simulator has no effect on the incident pulses (voltage, current or electric field). A comparable pair of reflected pulses (labeled B and C) emanate from the terminating resistor and the wall behind the absorbing material. However, the reflected pulses in the Harvard simulator are smaller (by about half) than those of the rhombic simulator for incident voltage pulses of the same magnitude. This is because the termination in the parallel-plate simulator has less effect on the SWR than that in the rhombic simulator: because of greater radiation, very little power can reach the termination.

The current pulse sequences have been measured at successive holes along two longitudinal lines on the underside of the top plate, one along the centerline and one close to the edge. The longitudinal distributions of the measured amplitudes of the incident current pulses in Figure 15 show that the amplitude decreases as the current pulse progresses. This behavior is similar to that in the rhombic simulator except close to the ends. Near the source
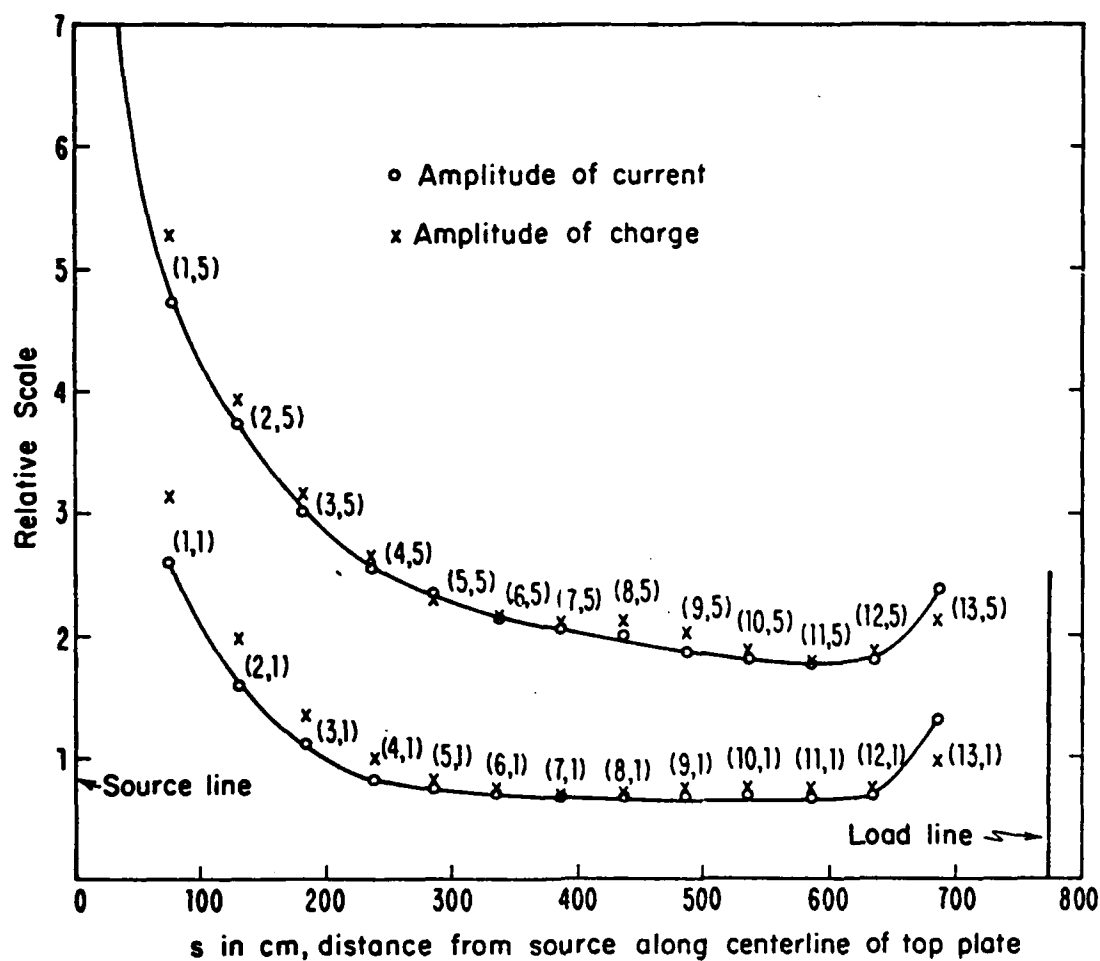
31

Figure 15. Longitudinal distribution of amplitudes of incident pulses measured along top plate of Harvard model simulator; $R_L = 90 \ \Omega$.

the decrease is much faster in the Harvard model simulator than in the rhombic simulator; near the load the amplitude increases instead of decreasing. The explanation of the differences is clear. What is actually measured is not the total current but the surface density of current which depends on the transverse dimensions. If consideration is given to the transverse dimensions -- which are very small near the two triangular ends -- the amplitude of the total current is close to that in the rhombic simulator where the current measured is on a wire of constant cross section. Transverse distributions of the current have been measured along several lines on both upper and lower sides of the top plate. The transverse distributions of the amplitudes of the incident current pulses in Figure 16 show that the amplitudes increase dramatically near the edge in complete agreement with earlier CW results. It is also significant that the current pulse that travels along the upper surface has an amplitude that is comparable and a distribution pattern that is similar to those of the pulse on the under surface. This is why the parallel-plate simulator radiates very significantly.

Measurements of the surface density of charge on the top plate were possible only after the development of a new, dual measurements technique to eliminate the severe systematic interference encountered. (This technique is discussed in more detail in Section VI.) The longitudinal and transverse distributions of the amplitudes of the charge are also shown in Figures 15 and 16 to permit a comparison with the current. In Figure 15 the amplitude distribution of the charge pulse is quite similar to that of the current pulse except at the two ends. Since the charge is proportional to the rate of change of the current, at the two ends of the top plate where the current amplitude changes rapidly, the charge pulse will be different. In Figure 16, the transverse distributions of the current and charge amplitudes are shown along the middle line (y = 0) of the simulator where the longitudinal distribution of the current amplitude is quite flat. Hence, the transverse distribution of the charge amplitudes is quite similar to that of the current.

The pulse sequences of the vertical electric field measured along the centerline of the ground plane in the Harvard EMP simulator are displayed in Figure 17. They are quite similar to those for the rhombic simulator shown in Figure 10. The incident electric-field pulse at the extreme left also decreases rapidly as it travels from near the source (Fig. 17, curve 1) to
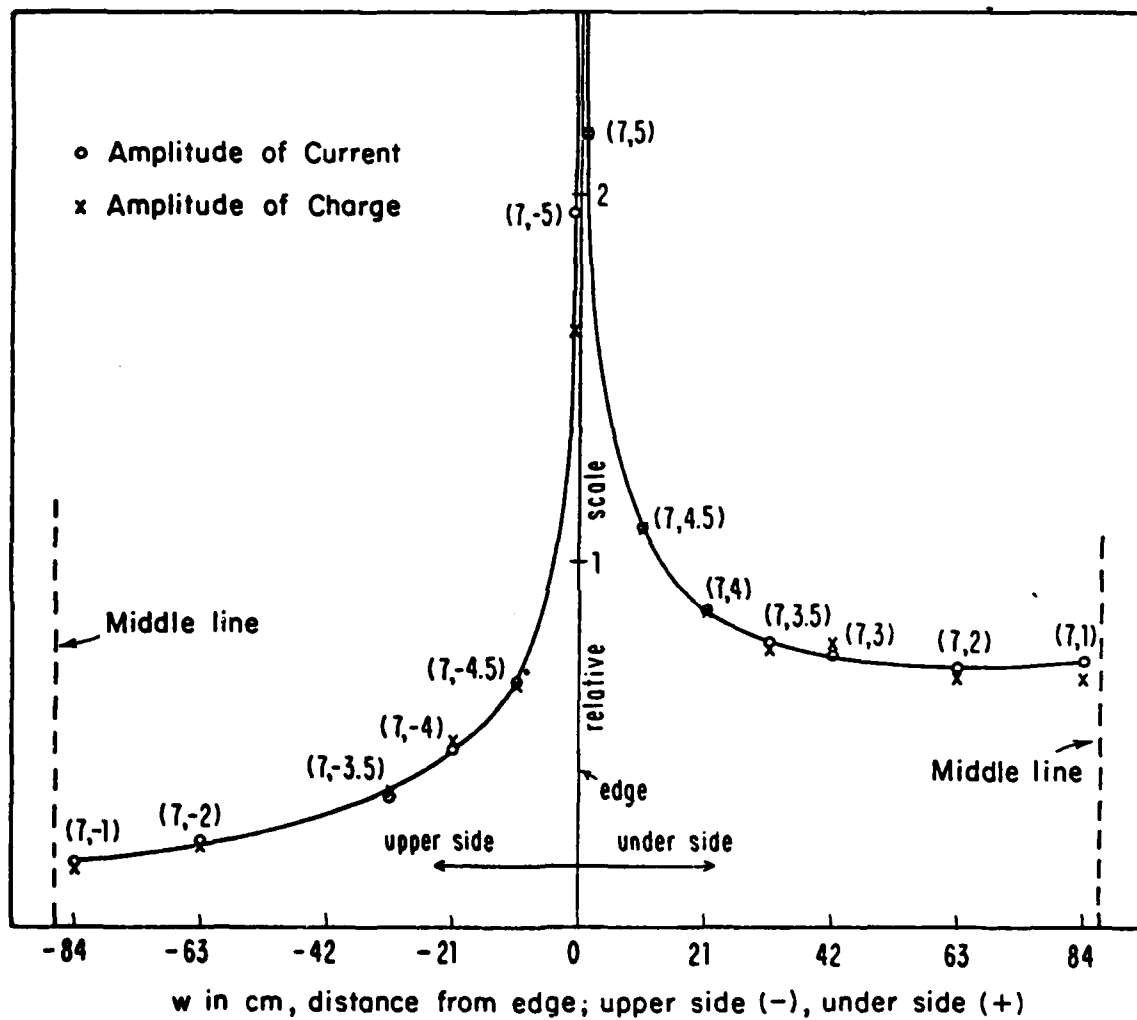
33

Figure 16. Transverse distribution of amplitudes of incident pulses measured along top plate of Harvard model simulator; $R_L = 90 \ \Omega$.
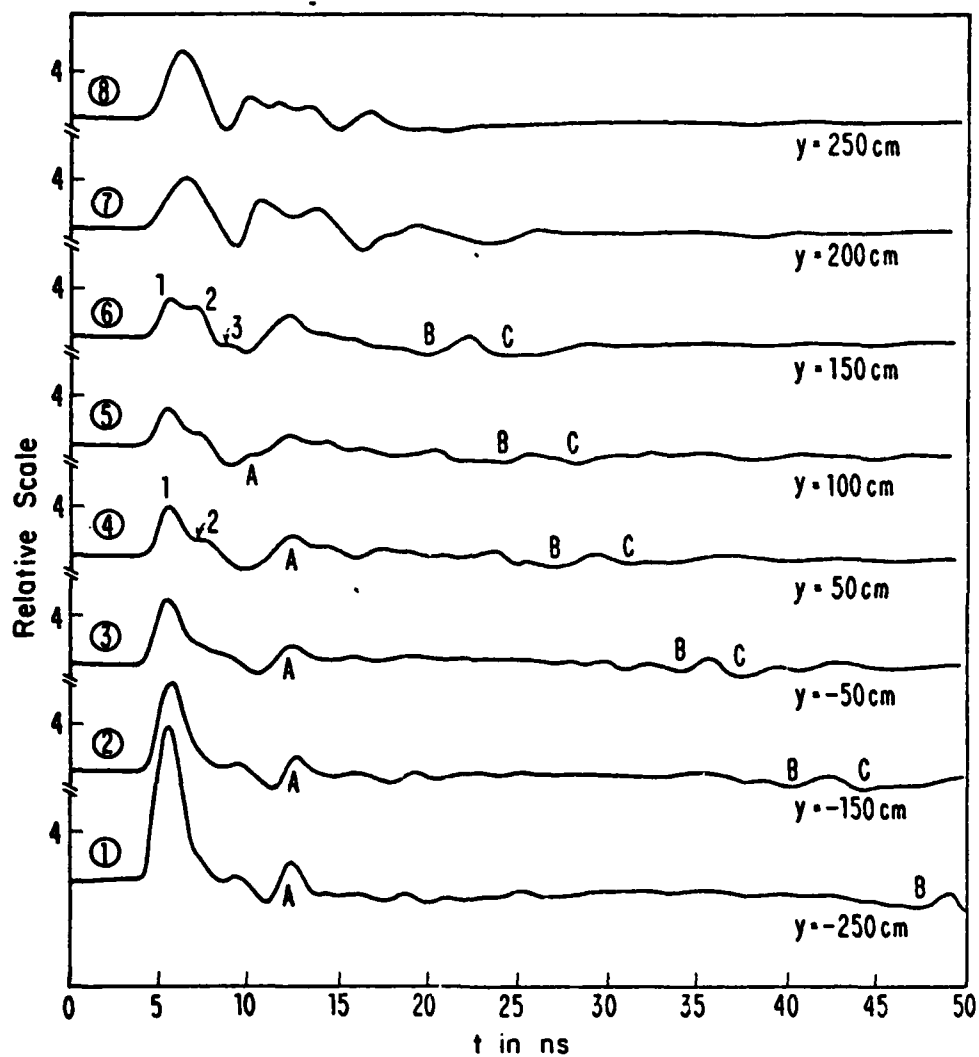
Figure 17. Vertical electric-field pulse sequences measured along centerline (x = z = 0) of ground plane in Harvard model simulator; R_L = 90 Ω.

35

near the load (Fig. 17, curve 8). As the probe is moved along the ground plane into the rear part of the simulator, a second pulse (Fig. 17, curve 4) and then a third pulse (Fig. 17, curve 6) are observed close to, but lagging behind the first pulse. Following these incident pulses, a strange negative pulse A (Fig. 17) is also observed, just as in the case of the rhombic simulator.

A physical picture of the mechanism of pulse excitation in the rhombic simulator was introduced earlier (Ref. 6) which shows that the electric field is actually excited by the current pulse as it traverses only a small part of the wire from which the subpulses are emitted in the forward direction. Following the same reasoning, a similar picture can be drawn for the Harvard model simulator; it is shown in Figure 18. With the help of this picture, the pulse sequences in Figure 17 can be explained. For the electric field on the front part of the ground plane near the source, only the current on the front sloping triangular plate can make a contributing forward emission. Therefore, the incident field pulse in this region is a single pulse (Fig. 17, curves 1 through 3) with the same decreasing amplitude observed in the rhombic simulator (Fig. 10). For the field beyond the working volume (Fig. 17, curve 4), the current on the top rectangular plate begins to make a contribution. In this case the major incident pulse (labeled 1) is emitted from the front triangular plate and the small pulse (labeled 2) is emitted from the current on the top rectangular plate. So far, the current on the rear triangular plate has made no contribution to the field since the emission from it is in the backward direction. For the field in the middle of the rear half of the ground plane, the current on a part of the rear triangular plate can contribute a forward emission, as shown in curve 6 of Figure 17, in which the major pulse 1 is from the current pulse in the front plate, pulse 2 is from the current pulse in the middle plate, and pulse 3 is from the current pulse in the rear plate. For the field near the load, these pulses are so close together that they form a single wide pulse, as shown in curves 7 and 8 of Figure 17.

With the help of the dual measurements technique, it is possible to measure the electric field in the working volume of the simulator. To measure the field in the space between the metal plates, the sensor has to be a dipole. This involves a matching problem with a balanced-to-unbalanced transformation.

Figure 18. Schematic diagram of the excitation of the electric-field pulse in the Harvard model simulator.

37

In the CW case, a balun is used which can be adjusted for a certain frequency. With pulse excitation, such a balun cannot work. It is for this reason that no measured data were shown of the electric-field pulse in the space above the ground plane in the study of the rhombic simulator. The horizontal distribution of the amplitude of the vertical electric-field (E_z) pulse on the z = 43 cm plane in the working volume is shown in Figure 19; the vertical distribution along the z-axis is shown in Figure 20. It is seen that the vertical electric-field pulse is quite uniform in the working volume. The amplitude does decrease slightly along the direction of travel (y-direction). Figure 20 also shows the vertical distribution of the amplitude of the longitudinal electric-field (E_y) pulse. This has a maximum near the middle of the space between the two parallel plates and zero on each plate. The amplitude at the maximum is only one-fifth to one-sixth as large as the amplitude of the E_z pulse. It follows that the electromagnetic field in the working volume is dominated by the vertical EMP with only a small longitudinal EMP. As in the CW case, the vertical electric-field pulse corresponds to a TEM mode while the longitudinal electric-field pulse corresponds to a TM mode. In general, it may be said that the nature of the incident electric-field pulse in the working volume of the Harvard model simulator is reasonably like an incident plane pulse.

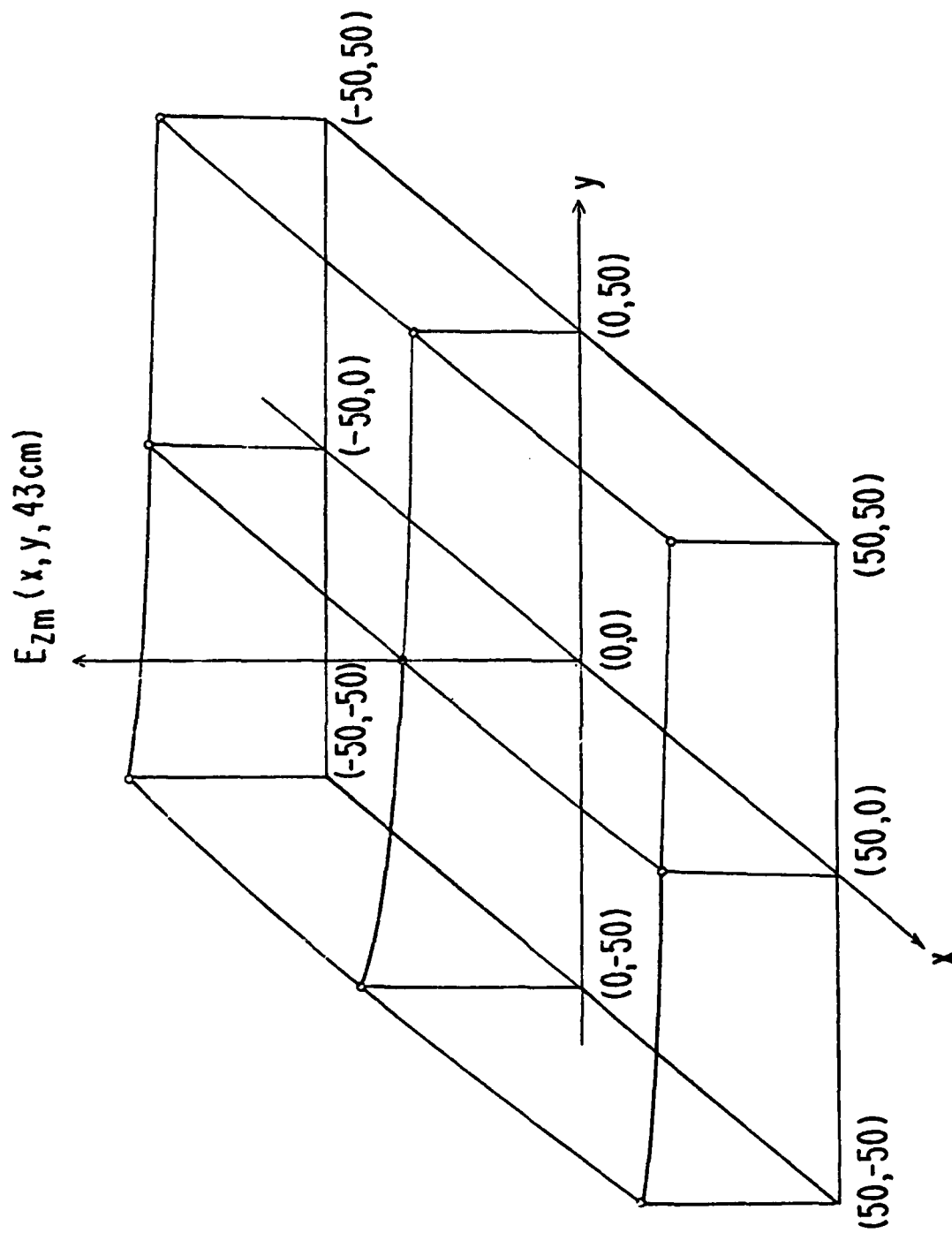Figure 19. Horizontal distribution of amplitude of vertical electric-field pulse on z = 43 cm plane in Harvard model simulator; R_L = 90 Ω.
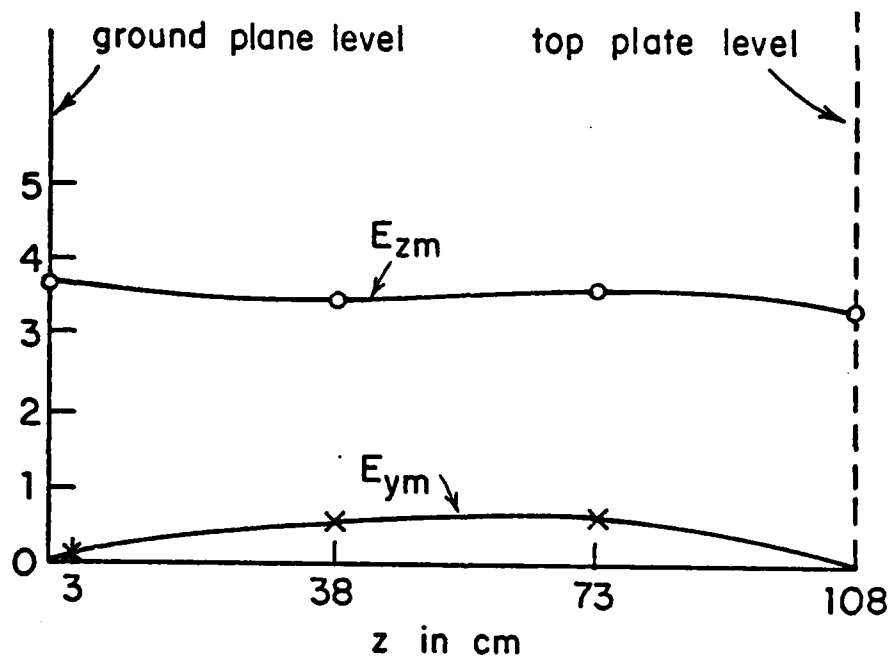
39

Figure 20. Vertical distribution of vertical (E_z) and longitudinal (E_y) electric-field pulses along z-axis in Harvard model simulator; $R_L = 90\ \Omega$.

VI. THE DUAL MEASUREMENTS TECHNIQUE;
ELIMINATION OF SLOWLY CHANGING BACKGROUND

In the experimental investigation of an EMP simulator under pulse excitation, all of the different measurements undertaken involve a systematic interference that is superimposed on the signal, partially obscures it, and degrades the accuracy of the measurement. At times the interference is so severe that the measurement becomes impossible. To eliminate such parasitic signals, a special dual measurements procedure has been developed (Ref. 8) which noticeably reduces the interference. The dual measurements procedure, in conjunction with a change in the sensor, can be used in a variety of measurements. To measure the electric field in the space between the plates, an electric dipole is used as the sensor. The dipole has a balanced output so the transmission line must be a parallel-wire line, a shielded twin line, or two coaxial lines. With pulse excitation, the resulting matching problem cannot be solved as in the CW case by using a balun. The balanced output of the dipole makes it necessary to connect one half of the dipole to the recording instrument, one half to an equivalent load. This arrangement solves only the problem of the balanced output of the dipole, not that of the interference. Because the two coaxial lines from the dipole to the digitizer pass through an area where the electromagnetic pulse exists, a significant current is induced on the outer conductor of each of the lines. The actual current reaching the recording instrument is the superposition of the signal current from one terminal of the dipole and the undesired interference current. The interference may be as strong or even stronger than the signal current. Because the coaxial cables are close together in their extension across the illuminated region, they carry the same induced current; this is important. If the two cables are disconnected and interchanged, a different waveform is observed: the signal current is now inverted (upside-down), but the interference is almost the same. Thus, if one of the two measured signals is subtracted from the other, the interference currents cancel while the signal current is doubled. The resulting difference curve is shown in curve 3 of Figure 21. A comparison with curves 1 and 2 (the two measured signals) shows that the interference current has been notably reduced and an even, clean signal current obtained. To cancel the interference current more exactly, the curves should be aligned before the subtraction takes place. It is important to keep
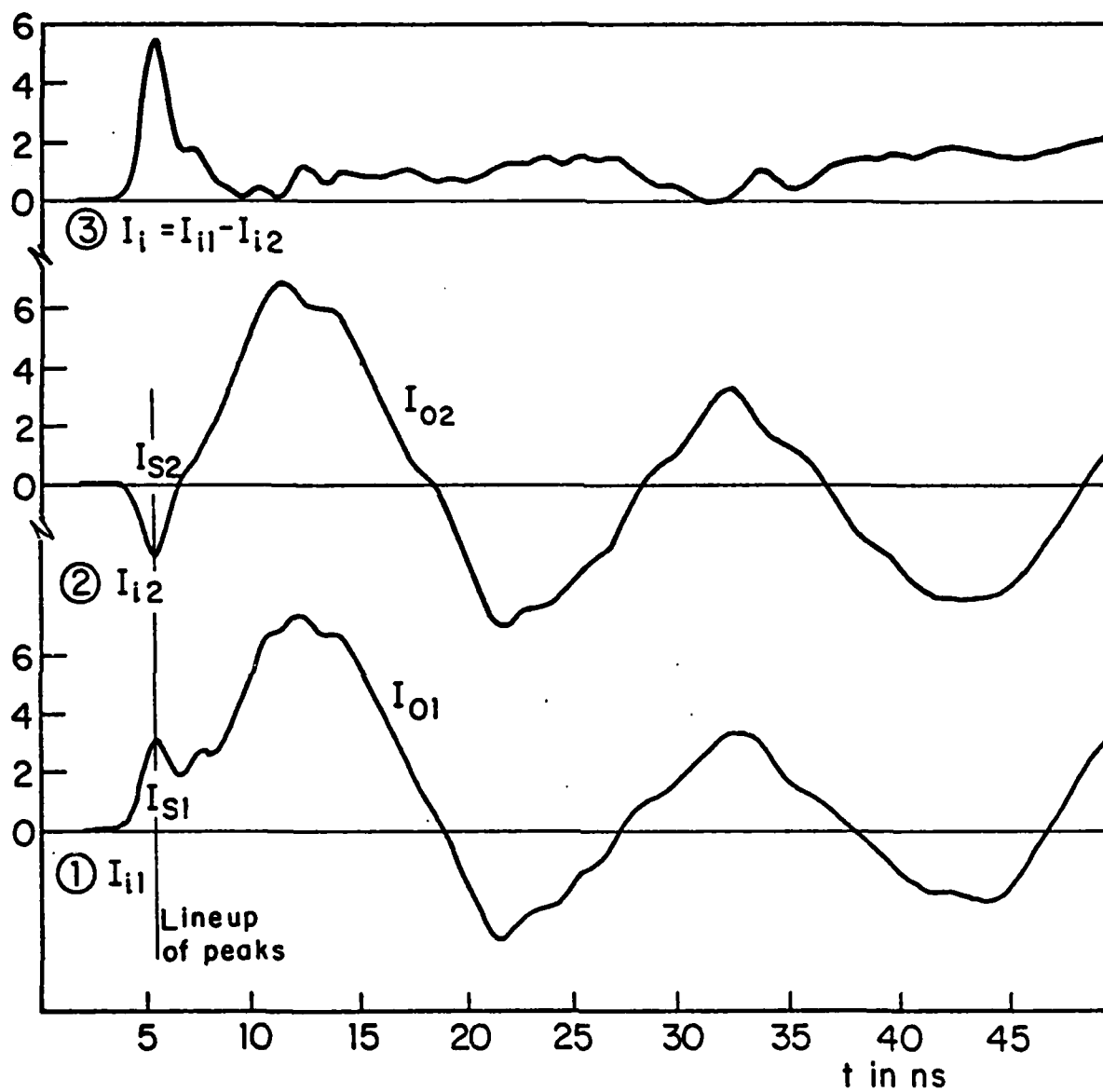
Figure 21. Induced currents due to electric field in working space as detected by each half of dipole and their difference.

the two coaxial lines as close together as possible and to maintain the physical layout unchanged during the dual measurements.

In other measurements (e.g., current and charge) in an EMP simulator, similar problems involving induced interference currents occur. Because different sensors are used instead of the dipole (e.g., loop or monopole), other methods are needed to produce a negative signal with the same interference. In current measurements, this can be accomplished with a magnetic dipole (two opposite loops) or simply by rotating the loop through 180 degrees and repeating the measurement. In the case of charge measurements using a monopole, it is not possible to rotate the monopole to obtain a negative signal or to use an electric dipole. The fact that the sign of the signal current cannot be reversed in the second measurement is not crucial. So long as the interferences are the same, a clean signal can be obtained if the relative magnitudes of the signal currents in the two measurements are made different. This can be achieved by making the two measurements with monopoles of different size. This latter method (changing the size of the sensor) can also be used to improve the data obtained from measurements of the electric field E_z on the ground plane of the simulator. E_z is detected by a moncpole on the metal ground plane connected by a coaxial line to the detecting instrument. Unlike the situation for the charge measurements on the top plate, the electric field under the ground plane is very weak and the interference is small. Curve 1 of Figure 22 shows E_z as detected by a monopole in the working volume. The interference contributes a small and slowly changing background to the signal, as shown by the dash-dot line. When use is made of the dual measurement procedure, this background disappears (Fig. 22, curve 3).
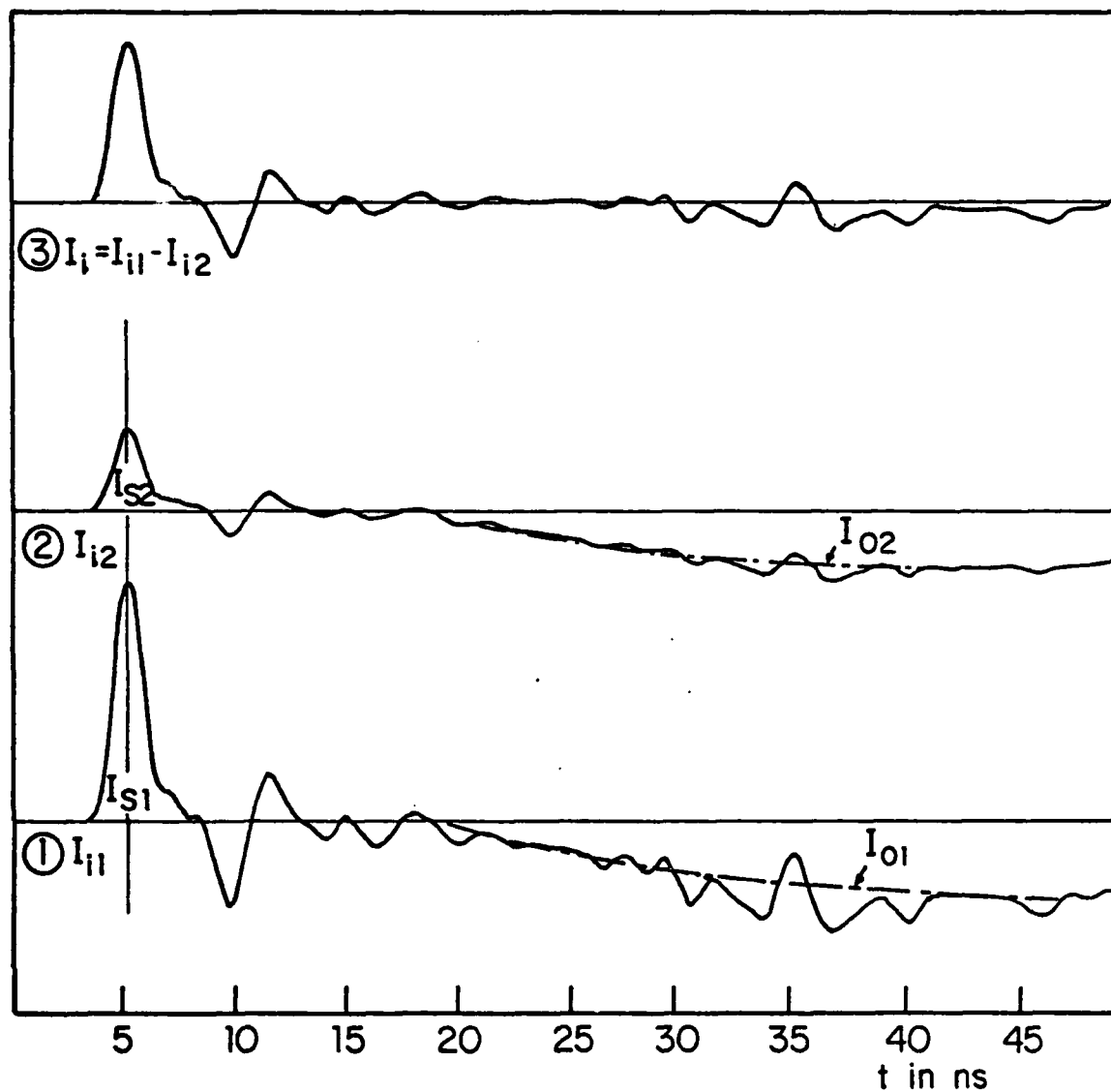
43

Figure 22. Induced currents due to electric field (E_z) on ground plane as detected by monopoles of different sizes and their difference.

44

VII. MATCHING BETWEEN SIMULATOR AND PULSE GENERATOR;
ELIMINATION OF PARASITIC PULSES

When an EMP simulator is excited by a single voltage pulse from the source at one end, the electric-field pulse within the simulator should consist of a similar single incident pulse (labeled E_{I0}) with a somewhat different shape, followed by a pair of small pulses (labeled B and C) reflected from the terminals of the simulator, as shown in curve 1 of Figure 23. Between the incident and reflected pulses, there should be no additional pulses. Actual measurements, however, have shown that there are many parasitic pulses between them. See, for example, curve 2 in Figure 23. After the main incident pulse (E_{I0}) there is a long tail (slowly changing background shown in dashed line) on which are superimposed many small pulses (labeled E_{I1}, E_{I2}, etc.). There is also a significant negative-positive pulse sequence (labeled A) to which numerous references have been made (Refs. 5 and 7). Since these unexpected parasitic pulses are very close to the main incident pulse E_{I0}, they may significantly affect an EMP test. It is, therefore, important to determine their origin and then to find ways to eliminate them.

Much effort has been expended to locate the sources of the parasitic pulses within the simulator, but without success. Since the development of the dual measurements procedure, the interference which caused the undesired slowly changing background has been eliminated (see Section VI), and the new curves for the electric-field, current, and voltage pulses are more accurate and clear. They reveal similar patterns of parasitic pulses, as shown in curves 1 through 3 in Figure 24. The output voltage pulse from the generator, however, shows a different pattern (Fig. 24, curve 4). When a 50-Ω high-frequency resistance instead of the simulator is connected directly to the generator, the incident voltage pulse sequence contains many small pulses following the main pulse, but the negative-positive pulse pair A is not present. Since pulse A has its origin in neither the generator nor the simulator, its only possible source is in the interaction between them. A detailed study has been made of the matching between an EMP simulator and its pulse generator (Ref. 9). The generator-simulator system is found to contain a chain of three circuits: (1) generator to feed point, (2) feed point to driving point, and (3) driving point to termination (see Figure 25). Due to the mismatching between these points, three sets of multiple reflections occur in the chain
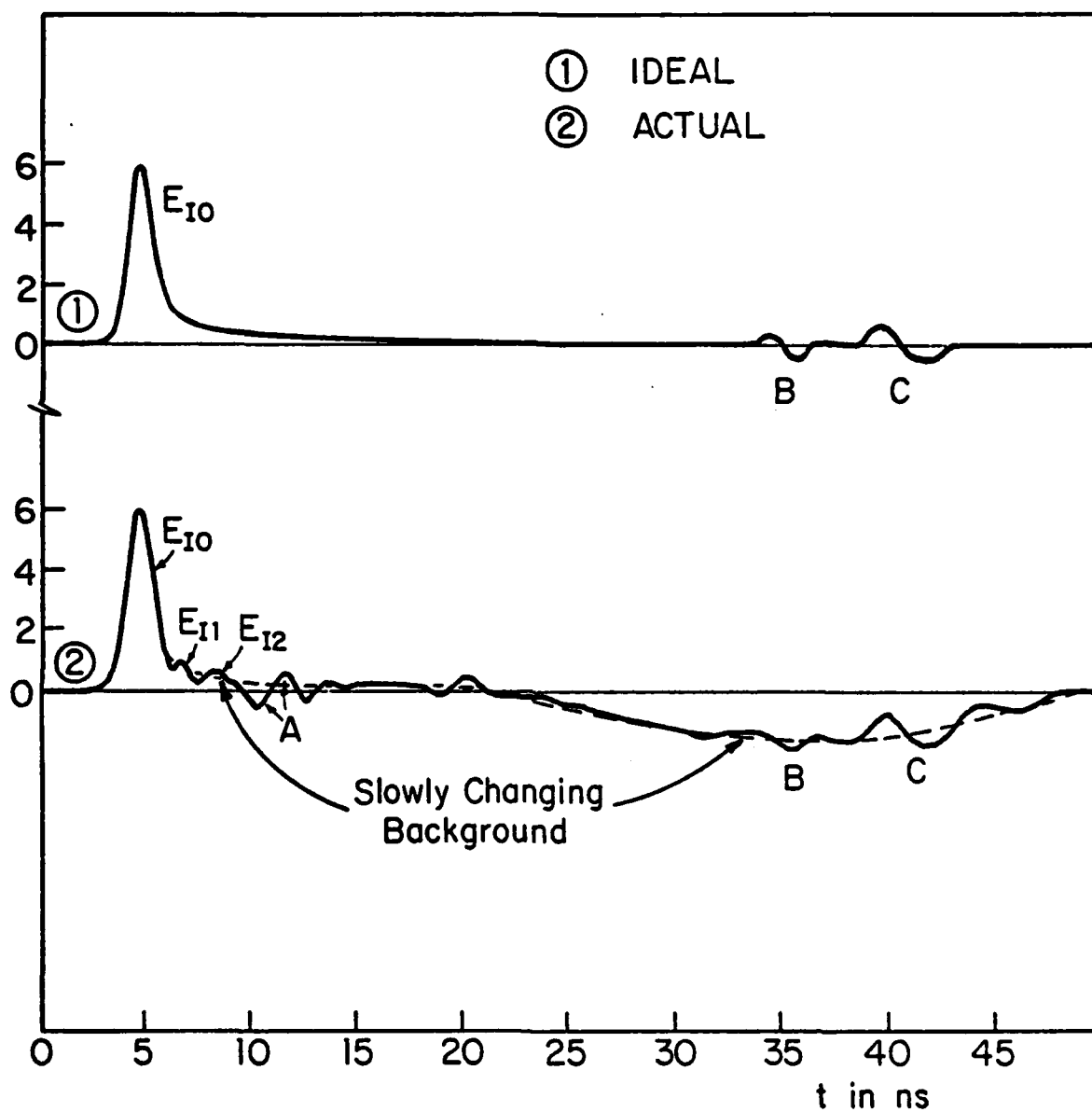
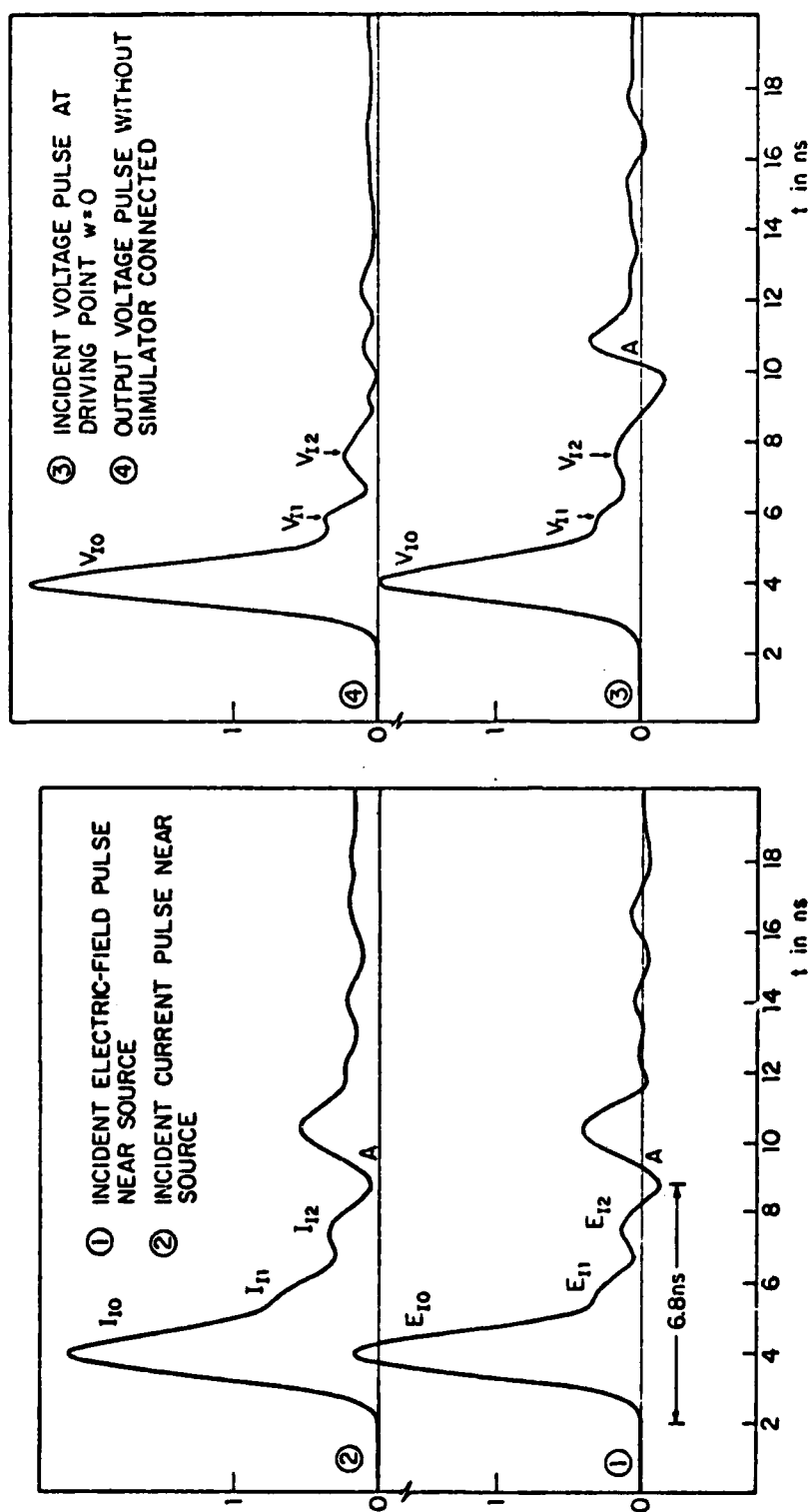Figure 23. Electric-field pulse sequence within simulator excited by single voltage impulse.

Figure 24. Comparison of incident pulses (electric-field, current and voltage) together with output voltage pulse from generator without simulator connected.

47
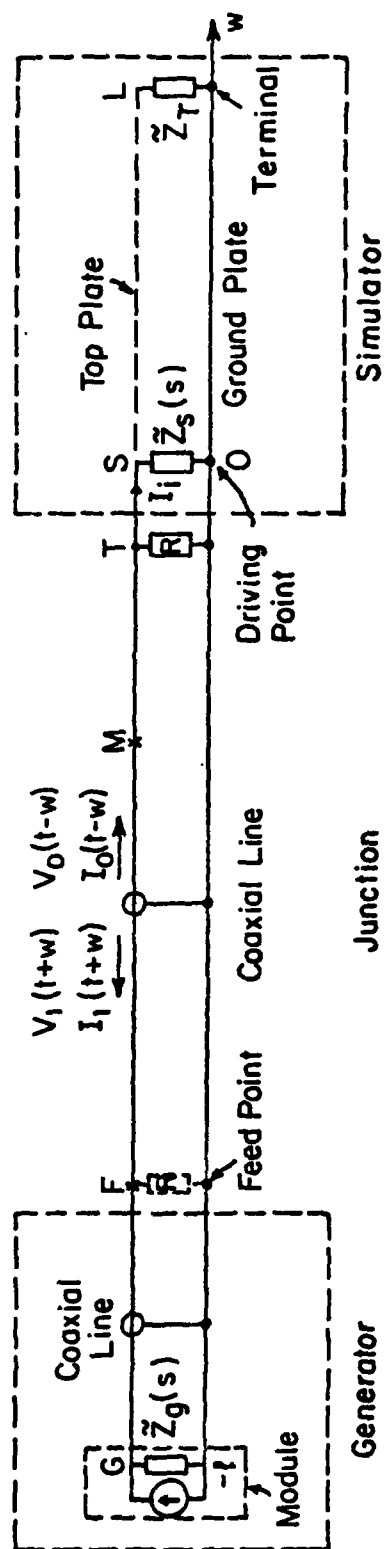
Figure 25.   Schematic diagram of generator-simulator system.

between the connections. The parasitic pulses B and C (Fig. 23) due to the multiple reflections between the termination and the driving point are not severe since they are small and are separated from the incident pulse. The negative-positive pulse sequence A (Fig. 23) is the first in a series of parasitic pulses due to the multiple reflections along the coaxial line between the feed point and the driving point of the simulator. They can be eliminated by matching at the driving point or by separating them from the main pulse by increasing the length of the connecting coaxial line. The third type of parasitic pulse is due to multiple reflections inside the generator along a short section of coaxial line between the feed point and the module which actually produces the signal. These parasitic pulses (labeled E_{I1}, E_{I2}, etc. in Fig. 23) can be eliminated by matching at the feed point by carefully choosing the coaxial lines on both sides of the feed point. All of the complicated features characteristic of the Harvard model simulator have now been explained and means found for their elimination.

VIII. THE QUASI-TRAVELING-WAVE EXPANSION METHOD FOR STUDYING TRANSIENT FIELDS

The complete theoretical and experimental understanding of the complicated physical phenomena associated with the transient electromagnetic field in a rhombic simulator and the demonstration that the rhombic and conventional parallel-plate simulators have similar properties are significant accomplishments. They provide a means for the systematic evaluation and possible improvement of conventional simulators and supply the basic theory and experimental procedures for the definitive study of the crucial obstacle-simulator interaction. This advance in knowledge has been enhanced further by the derivation of a new solution of the integral equation for the current in a cylindrical conductor in the time domain (Ref. 10). This new quasi-traveling-wave expansion method is based on the traveling property of the source function in the Hallén-type equation. It is suitable for use with antenna and scattering problems associated with long flat bodies (e.g., EMP simulators) on the surface of which the vector potential can be expected to propagate approximately as a traveling wave.

Transient radiation or scattering can be studied in the frequency or the time domain. In early work information about transients was obtained by Fourier transformation of solutions in the frequency domain. Since transient phenomena involve new features which are difficult to treat, interpret or measure in the traditional continuous-wave manner, new methods have been developed to obtain time-domain solutions more directly, accurately and efficiently. Since the solutions of only a few transient problems can be expressed in closed form, the time-dependent integral equation is solved by expansion techniques supplemented by numerical computation. When the testing-function series is in the complex frequency plane, the available approaches include the low-frequency method with power series, the singularity expansion method with a singularity series, the high-frequency method with asymptotic series, and an eigenmode expansion method. With excitation by a single short pulse, the response (current) is a pulse sequence which includes the primary pulse and reflected pulses. In the approaches listed above, the response functions are determined in their entirety. There are often situations when it would be advantageous to treat the response functions (current) separately, i.e., to solve for the primary and reflected current pulses individually. Some reasons for the individual treatment include:

(1) In many cases a knowledge of only a part of the complete pulse sequence is of interest. For example, in EMP generation and testing, only the primary pulse is of interest. (To evaluate the primary EMP in the working volume, only information on the primary current pulse on the front plate is needed.)

(2) The structure of the entire system is too complicated to permit the evaluation of the complete pulse sequence. However, since the electromagnetic field interacts with different parts of the structure during different time intervals, it is possible to solve for the individual pulses in the sequence with different considerations of the boundary conditions. For instance, when considering the early response of the primary pulse, only the parts of the structure near the source need to be taken into account. This is a much simpler problem.

(3) Theoretically, the response function can be expanded into any infinite series but, practically, only a finite number of terms can be taken into account. As a consequence, questions of accuracy and efficiency arise. If the testing function has little relation to the response function, the use of a limited number of terms is not likely to be a good representation. There are two important states in electromagnetic phenomena: the state of resonance (standing wave) and the traveling wave. When the excited system is near resonance, the singularity expansion procedure is effective. However, if the response of the system is a traveling wave on a long terminated transmission line, EMP simulator, etc., a traveling-wave-like testing function should be used.

The ideas underlying the determination of transient responses can be summarized as follows:

(1) Because of the nature of the multiply reflected pulse sequence, the source function $F(t,z)$ and the response function $I(t,z)$ are expanded into individual pulse pairs (F_m, I_m) to obtain a recurrence integral equation. This can be solved for the pulse pair (F_m, I_m) sequentially.

(2) $I_m(t,z)$ is a rapidly changing function of both t and z. The principal idea for solving I_m rests on the separation of the z-dependent and z-independent parts so that the latter can be removed from under the sign of integration. Based on the traveling-wave nature of $F_m(t \pm z)$, the part

51

that changes rapidly with z is absorbed into $T = t \pm z$ so that the remaining z-dependent part of $I_q(t,z)$ is a slowly changing function of z, i.e., a quasi-traveling wave.

(3) The second major z-dependent part of the quasi-traveling wave, $I_q(T,z)$, has been drawn out by introducing the amplitude function $A(z)$ which is defined by a smoothing condition which assures that the shape function $H(T,z)$ has little dependence on z.

(4) Since the main and tail parts of the pulse have different z-behaviors, they are separated and determined sequentially. This simplifies the equations to be solved and demonstrates the causality of the response.

(5) The boundary conditions are supplemented by the addition of coupling terms which change the z-behavior of the current near the boundary. A further separation is then carried out to obtain equations that can be solved by adding adjustable terms, using different amplitudes, or iterating directly.

The solution for the current is approximate but accurate. Even for the first-order solution, the error is less than 1 percent except near turning points (driving point for I_0, endpoints for I_m) where the maximum error is less than 5 percent. Still greater accuracy can be obtained with higher-order solutions. The form of the solution provides physical insight in terms of the amplitude, the shape, and the tail of a pulse, and the transmission, admittance, and reflection functions. These physical quantities are useful for studying specific aspects of the response such as the amplitude decay, the change in shape, or the complex input admittance.

IX. CONCLUSION

The researches described in this final report provide a complete theoretical and experimental understanding of the operation of the rhombic simulator and a closely correlated experimental study of the Harvard metal-plate simulator. In particular, the nature of the electromagnetic field in the working volume is described when this is empty. The study of currents and charges induced on obstacles located in the working volume has been limited to vertical tubular cylinders, crossed cylinders, and cylinders with a cross consisting of a metal plate under CW operation with one polarization. The important and difficult final problem of induced currents and charges on extended obstacles like aircraft arbitrarily located with respect to the direction of incidence and the polarization of the electromagnetic field remains to be investigated for both CW and pulse operation.

REFERENCES

1. King, R. W. P., and Blejer, D. J., "The Electromagnetic Field in an EMP Simulator at a High Frequency," IEEE Trans. Electromagn. Compatibil., EMC-21, pp. 263-269, August 1979.

2. King, R. W. P., Blejer, D. J., and Wu, T. ⌐., "Standing Waves and Notches in an EMP Simulator and Their Reduction," IEEE Trans. Electromagn. Compatibil., EMC-23, pp. 80-87, May 1981.

3. King, R. W. P., "Induced Charges on a Cylinder Excited by Standing and Traveling Waves in an EMP Simulator," IEEE Trans. Electromagn. Compatibil., EMC-24, pp. 287-291, May 1982.

4. Kao, C. C., "Three-Dimensional Electromagnetic Scattering from a Circular Tube of Finite Length," J. Appl. Phys., 40, pp. 4732-4740, November 1969.

5. Shen, H. M., King, R. W. P., and Wu, T. T., "An Experimental Investigation of the Rhombic EMP Simulator under Pulse Excitation," IEEE Trans. Electromagn. Compatibil., EMC-25, pp. 40-46, February 1983.

6. Shen, H. M., King, R. W. P., and Wu, T. T., "Theoretical Analysis of the Rhombic Simulator under Pulse Excitation," IEEE Trans. Electromagn. Compatibil., EMC-25, pp. 47-55, February 1983.

7. Shen, H. M., King, R. W. P., and Wu, T. T., "An Experimental Investigation of the Parallel-Plate EMP Simulator with Single-Pulse Excitation," IEEE Trans. Electromagn. Compatibil., EMC-25 (scheduled to appear in August 1983 issue, Part II).

8. Shen, H. M., King, R. W. P., and Wu, T. T., "The Dual Measurement Procedure for Eliminating Systematic Interference," (submitted for publication). IEEE Trans. Electromagn. Compatibil.

9. Shen, H. M., King, R. W. P., and Wu, T. T., "The Matching Between an EMP Simulator and the pulse Generator," (submitted for publication). IEEE Trans. Electromagn. Compatibil.

10. Shen, H. M., "The Quasi-Travelling-Wave Expansion Method for Direct Time-Domain Solution," (submitted for publication). IEEE Trans. Electromagn. Compatibil.

END

FILMED

9-83

DTIC